signal ratio (FISH score) >2.2.[14] Histological grades were assessed according to the criteria of Elston and Ellis.[4] The Ki-67 immunoreactivity was evaluated by examining high-power fields and counting 1000 tumor cells in the hot spots.[15] In addition, the presence or absence of lymphovascular invasion was determined according to *Rosen's Breast Pathology*.[12] Intrinsic subtypes were classified according to the St Gallen international expert consensus on the primary therapy of early breast cancer 2011[16] as follows: luminal A was ER and/or PgR positive, HER2 negative, and Ki-67 low (<14%); luminal B was either ER and/or PgR positive, HER2 negative and Ki-67 high, or ER and/or PgR positive, any Ki-67, and HER2 overexpressed or amplified; the HER type was HER2 overexpressed or amplified and ER and PgR absent; and triple negative was ER, PgR and HER2 negative.

We compared mammographic findings, including mass shape, margin, density, calcification, FAD, and architectural distortion, with the histopathological characteristics of the tumors, including intrinsic subtype, histological grade, lymphovascular invasion, and the Ki-67 labeling index.

Statistical analysis. To compare mammographic findings with histopathological findings, multivariate analysis was used. All analyses were performed using SPSS version 10.0 (SPSS Inc., Chicago, IL, USA), with $P < 0.05$ taken to indicate significant differences.

Results

Comparison of mammographic findings with intrinsic subtype. Figure 2 summarizes the results of the numbers and ratios of each mammographic finding according to intrinsic subtype. In the luminal A group, significant differences were identified between masses that were irregular and lobular or round ($P = 0.017$ and $P = 0.024$), between those that had speculated and indistinct or microlobulated margins ($P < 0.001$ and $P = 0.001$), between those showing amorphous and pleomorphic calcification ($P = 0.044$), and between the presence and absence of architectural distortion ($P = 0.002$). In the HER group, significant differences were identified between masses that were irregular and oval or round ($P = 0.009$ and $P < 0.001$), between masses that were lobular and round ($P = 0.021$), and between those that had spiculated and microlobulated margins ($P = 0.005$). In the triple negative group, significant differences were identified between masses that had spiculated and

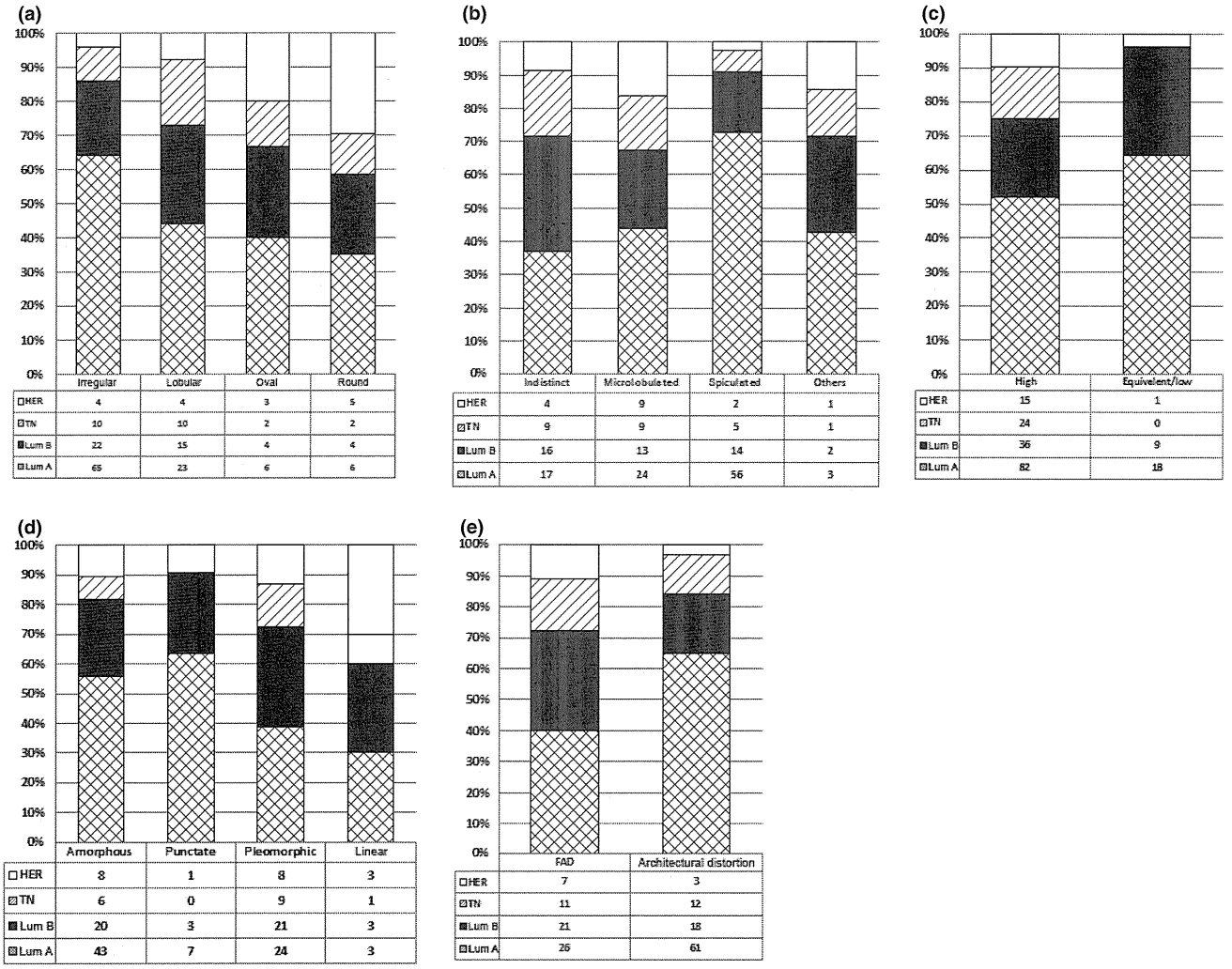

Fig. 2. Correlation between mammographic findings and intrinsic subtype: (a) mass shape, (b) margin, (c) density, (d) calcification shape, and (e) focal asymmetric density (FAD) and architectural distortion. HER, human epidermal growth factor receptor; TN, triple negative; Lum A, luminal A; Lum B, luminal B.

© 2011 Japanese Cancer Association

indistinct margins ($P = 0.027$), as well as between those identified as having high and equivalent or low density ($P = 0.027$).

Comparison of mammographic findings with histological grade. Figure 3 summarizes the results of the numbers and ratios of each mammographic finding according to histological grade. There were significant differences between irregular and lobular or oval mass shape in Grade 3 ($P < 0.001$ for all). Furthermore, in Grade 1 tumors, significant differences were found between with an indistinct and microlobulated or spiculated periphery ($P = 0.030$ and $P = 0.003$), between those with spiculated and indistinct or microlobulated margins ($P < 0.001$, respectively), between those identified as high and equivalent or low density ($P = 0.047$), and between those with a linear and amorphous calcification shape ($P = 0.027$).

Comparison of mammographic findings with lymphovascular invasion. Figure 4 summarizes the results for the numbers and ratios of each mammographic finding according to lymphovascular invasion. There were significant differences between oval and irregular or round mass shape ($P = 0.008$ and $P = 0.034$), between microlobulated and indistinct periphery ($P = 0.014$), between punctate and amorphous or pleomorphic calcification shape ($P = 0.030$ and 0.038), and between presence and absence of architectural distortion ($P = 0.027$).

Comparison of mammographic findings with the Ki-67 labeling index. Figure 5 summarizes the results of correlations between mammographic findings and the Ki-67 labeling index. The Ki-67 labeling index according to mass shape was 15.74 ± 6.21 for irregular masses, 38.82 ± 13.10 for lobular masses, 36.22 ± 15.75 for oval masses, and 37.85 ± 14.95 for round masses. According to mass periphery, the Ki-67 labeling index was 35.80 ± 28.51, 34.56 ± 29.76, 11.73 ± 10.86, and 27.50 ± 24.75 for tumors with indistinct, microlobulated, spiculated, and ''other'' margins, respectively. For tumors with a high and equivalent or low mass density, Ki-67 labeling index was 27.68 ± 26.75 and 13.14 ± 14.10, respectively. Tumors that showed amorphous, punctate, pleomorphic, and linear calcification had a Ki-67 labeling index of 24.55 ± 7.58, 26.00 ± 18.27, 24.68 ± 9.43, and 16.00 ± 17.23, respectively. In tumors without and with architectural distortion, the Ki-67 labeling index was 22.27 ± 8.64 and 25.02 ± 7.43, respectively. There were significant differences between irregular and lobular or round ($P < 0.001$ and $P = 0.014$), spiculated and indistinct or microlobulated ($P < 0.001$ for all), and high and equivalent or low density ($P = 0.018$) groups. A trend for a positive correlation was detected between irregular and oval mass shape, but the difference did not reach statistical significance ($P = 0.062$).

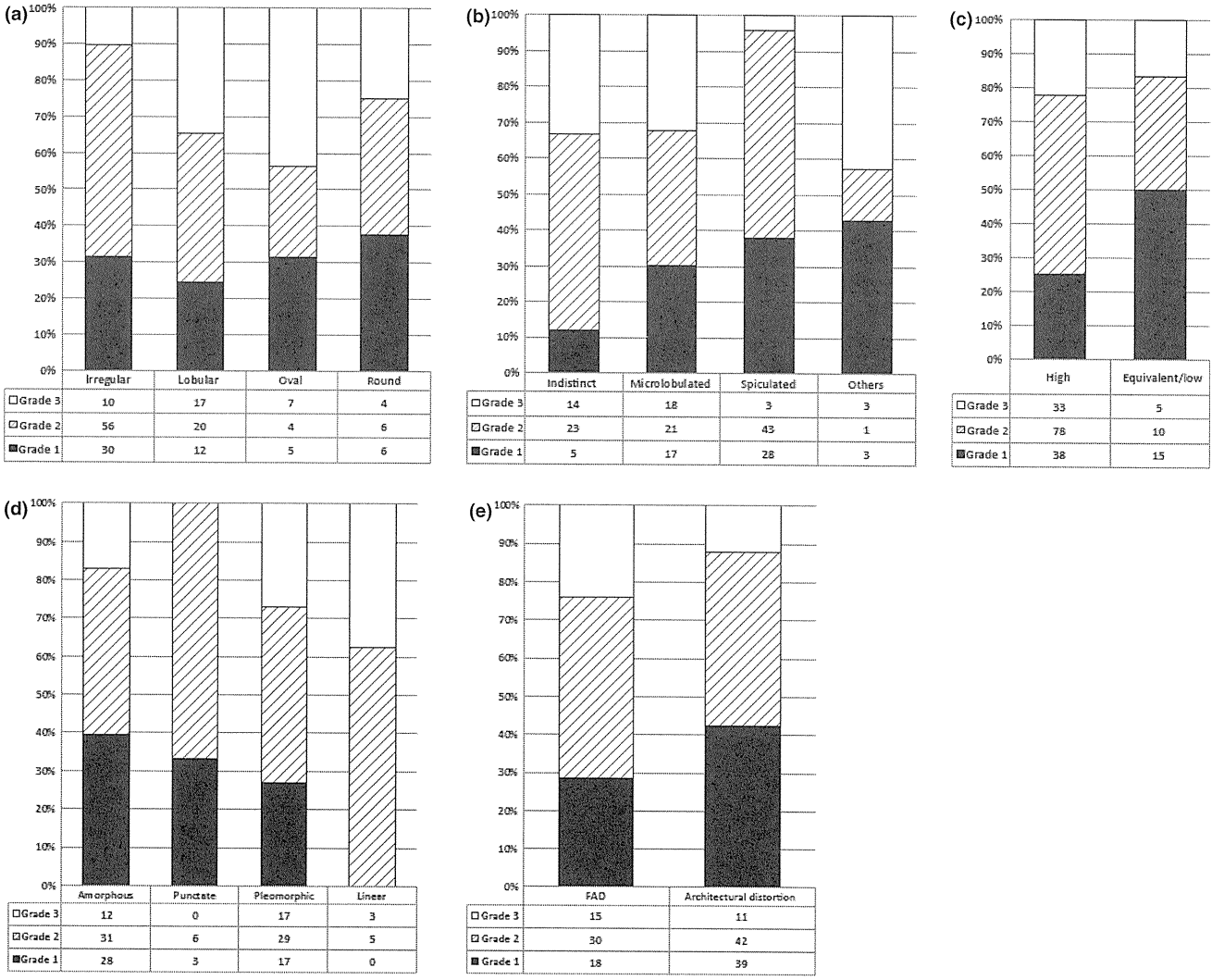

Fig. 3. Correlation between mammographic findings and histological grade: (a) mass shape, (b) margin, (c) density, (d) calcification shape, and (e) focal asymmetric density (FAD) and architectural distortion.

doi: 10.1111/j.1349-7006.2011.02088.x
© 2011 Japanese Cancer Association

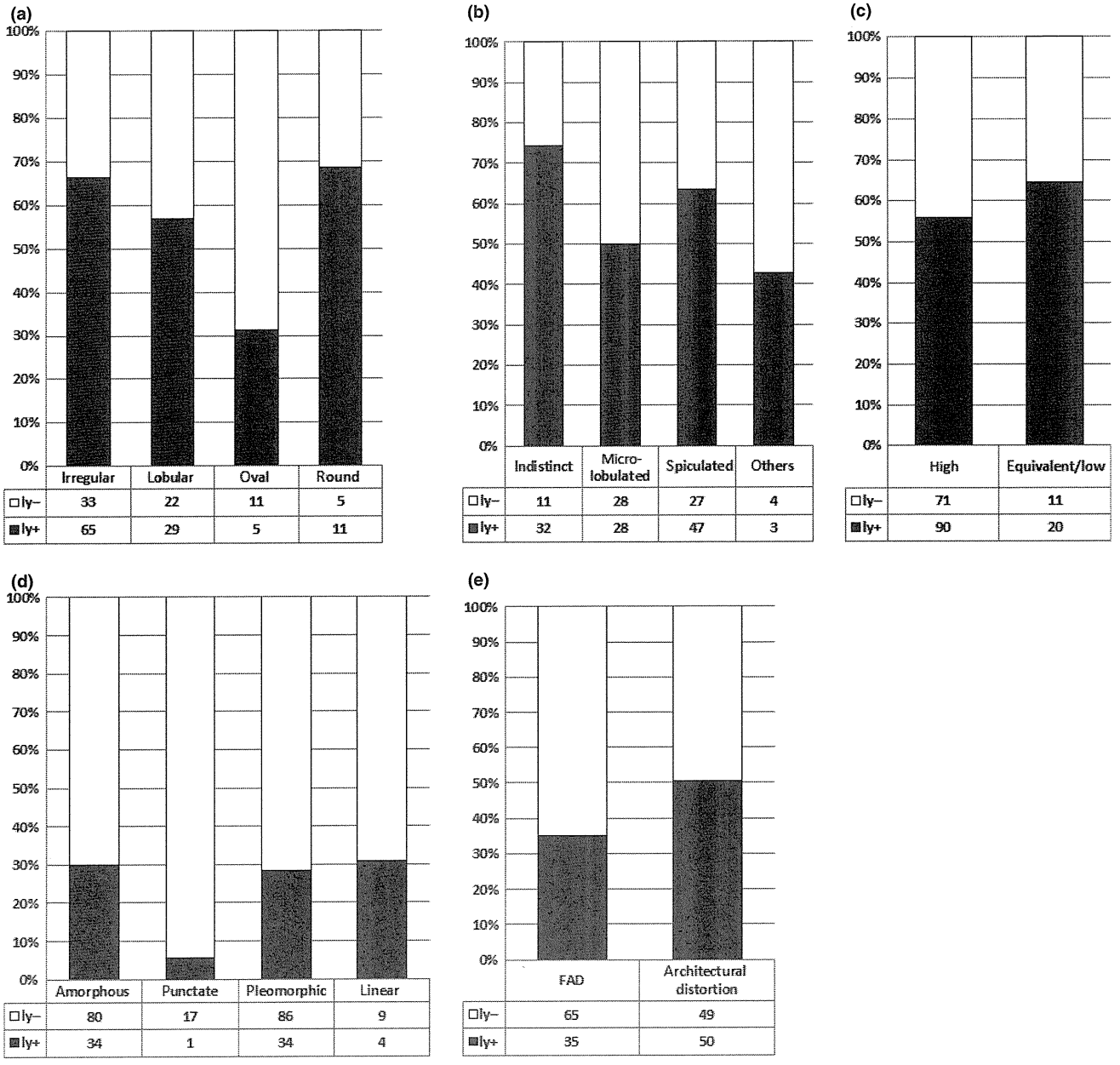

Fig. 4. Correlation between mammographic findings and lymphovascular invasion: (a) mass shape, (b) margin, (c) density, (d) calcification shape, and (e) focal asymmetric density (FAD) and architectural distortion. ly–, no lymphovascular invasion; ly+, lymphovascular invasion.

There were no significant differences according to calcification shape and the presence of architectural distortion.

Discussion

Histological grade is well known to have a strong correlation with clinical outcome in patients with breast cancer.[4] Accumulating clinical evidence suggests that prognostic factors influencing breast cancer extend beyond the traditional tumor histological grade.[17] Several factors, including ER expression, HER2 status, and lymphovascular invasion, have been clearly demonstrated in recent years to contribute significantly to the management and subsequent prognosis of patients with breast cancer.[7,18] Therefore, an accurate correlation between mammographic findings and their corresponding histopathological features is considered most important in mammographic evaluation. Mammographic findings may provide insights into pathological and biological features, including tumor cell characteristics, histological grade, and cell proliferation. We attempted to determine which finding is more relevant with regard to the newly defined subtype of breast carcinoma cells. Therefore, the purpose of the present study was to evaluate the correlation between mammographic findings (e.g. mass shape, margin, density, calcification shape, FAD, and the presence of architectural distortion) with intrinsic subtype, histological grade, lymphovascular invasion, and the Ki-67 labeling index in breast cancer patients.

Several previous studies evaluated the correlation between mammographic findings and histopathological characteristics in individual patients.[8,19–21] A number of independent groups demonstrated that masses with a spiculated periphery were associated with a good outcome in patients.[19,20] Conversely,

© 2011 Japanese Cancer Association

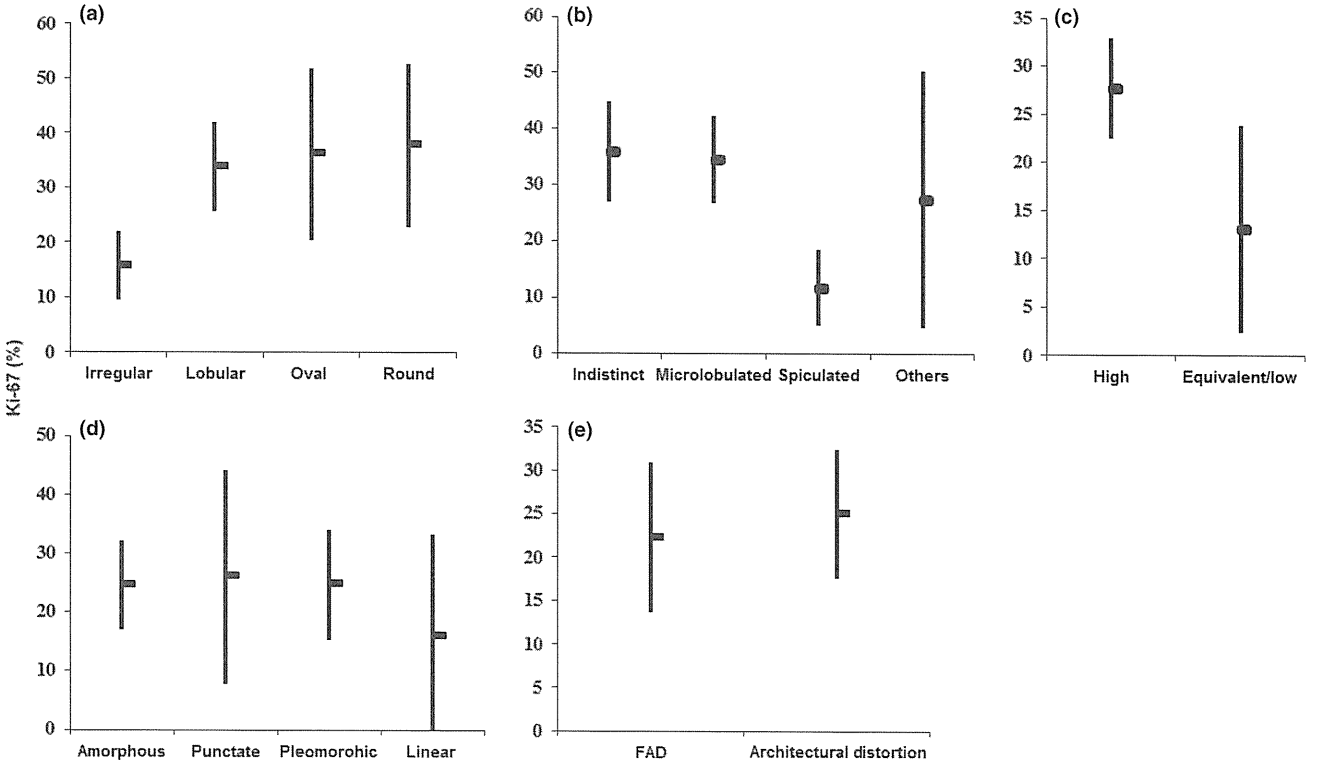

Fig. 5. Correlation between mammographic findings and Ki-67 labeling index: (a) mass shape, (b) margin, (c) density, (d) calcification shape, and (e) focal asymmetric density (FAD) and architectural distortion.

well-defined masses were associated with triple-negative breast cancer.[8,21] The results of the present study demonstrate that is a higher incidence of lower histological grade in masses with an irregular shape and/or spiculated margins, although a higher histological grade is not necessarily associated with irregular mass shape or spiculated margins. In addition, correlation of mammographic findings with the intrinsic subtype demonstrated that irregular mass shape and/or spiculated margin masses were significantly more frequently detected in luminal A breast cancers than in the other subtypes in this cohort of Japanese patients. However, oval and round mass shape and/or indistinct and microlobulated margin masses were significantly more frequently detected in triple-negative breast cancers or HER breast cancers. As for architectural distortion, the ratio of architectural distortion was significantly higher in luminal A cases and also tended to be associated with histological Grade 1. Together, these results suggest that poorly differentiated breast carcinoma cells are associated with good histological grade and luminal A subclassification. However, well-differentiated carcinoma cells are associated with adverse clinical grading and negative ER status.

Previous studies have demonstrated that these differentiations were related somewhat with adhesion factors.[22,23] Loss of adhesion factors in carcinoma cell is considered to play a role in the characteristic histological appearance of invasive carcinoma as loosely dispersed linear columns of cells and a typical discrete mass.[22] This more diffuse infiltrative pattern may explain some of the typical imaging appearances of tumors, such as spiculation and distortion.[22] In addition, adhesion factors are correlated with high histologic grade.[23] Therefore, adhesion factors may be considered to be correlated with the results of the present study in that spiculated breast cancers have a good clinical outcome and histological Grade 1. However, it is also true that numerous biological mechanisms underlying the association between the process of infiltration and histopathological characteristics remain unknown and that further investigations are required to confirm interpretation of mammography in terms of the biological and histopathologic characteristics of tumors.

To the best of our knowledge, this is the first study to compare mammographic findings with the Ki-67 labeling index and histopathological lymphovascular invasion. The results of the present study demonstrated that there was a higher incidence of a lower Ki-67 labeling index in tumors with an irregular mass shape, spiculated periphery, and equivalent or low mass density. Irregular mass shape and a spiculated periphery are well-known predictors of malignancy, but the results of the present study seem to suggest that findings of irregular shape and a spiculated periphery are relatively good prognostic predictors in terms of the Ki-67 labeling index. In addition, the results of the present study demonstrate that lymphovascular invasion was significantly greater in cases in which there was architectural distortion; however, the incidence of lymphovascular invasion was not significantly higher in spiculated masses. These results all suggest that the correlation between findings of radiological dist ortion and the mechanisms of lymphovascular invasion remain unknown and further investigations are required.

We also examined the correlation between mammographic calcification shape and histopathological characteristics. Previous studies have reported that triple-negative breast cancers are more likely to exhibit comedo calcifications.[8] In addition, the high frequency of comedo calcification in triple-negative breast cancers may represent a consequence of high histologic grade.[8] The presence of mammographic comedo calcification has also been reported to be associated with a poor prognosis in small screening-detected invasive cancers.[19] The results of the present study also demonstrate that non-necrotic calcifications, including amorphous and punctate calcification, are associated with a higher ratio of luminal A cases, whereas necrotic calcifications, including pleomorphic and linear calcification, were

doi: 10.1111/j.1349-7006.2011.02088.x
© 2011 Japanese Cancer Association

associated with a higher ratio of HER breast cancers. In addition, necrotic calcifications tended to be associated with a higher histological grade than non-necrotic calcifications. Therefore, the results suggest that the type of calcification may become a prognostic factor for breast malignancies.

We noted significant differences in the mammographic features of different primary breast cancer immunophenotypes in the present study. Stratifying the mammographic features according to immunophenotypes reveals distinct differences among cancer subtypes. However, the limitations of the present study include that fact that the study was retrospective in nature and was performed in a single institute, namely Tohoku University Hospital. Therefore, further investigations are needed, including analysis in several different institutions to further refine the new mammographic criteria. Biological and histopathological differences may result in imaging differences that may help us better understand the development of breast cancer. These proposed mammographic diagnostic criteria based on biological characteristics may contribute to a more accurate prediction of the biological behavior of breast malignancies.

Acknowledgments

The authors thank medical technologist Mr Masahiro Sai for his excellent technical assistance for mammography. The authors also thank medical technologist Ms Yayoi Takahashi for excellent technical assistance with the immunohistochemical staining. This work was supported, in part, by a Grant-in Aid from Kurokawa Cancer Research Foundation.

Disclosure Statement

The authors have no conflict of interest.

References

1 Nystrom L, Rutqvist L, Wall S *et al.* Breast cancer screening with mammography; overview of Swedish randomized trials. *Lancet* 1993; **341**: 973–8.
2 Tabar L, Vitak B, Chen HH *et al.* Beyond randomized controlled trials: organized mammographic screening substantially reduces breast carcinoma mortality. *Cancer* 2001; **91**: 1724–31.
3 Carter CL, Allen C, Henson DE. Relation of tumour size, lymph node status, and survival in 24,740 breast cancer cases. *Cancer* 1989; **63**: 181–7.
4 Elston CW, Ellis IO. Pathological prognostic factors in breast cancer. I. The value of histological grade in breast cancer: experience from a large study with long-term follow-up. *Histopathology* 1991; **19**: 403–10.
5 Lee AHS, Pinder SE, Macmillan RD *et al.* Prognostic value of lymph vascular invasion in women with lymph node negative invasive breast carcinoma. *Eur J Cancer* 2006; **42**: 357–62.
6 Bauer KR, Brown M, Cress RD *et al.* Descriptive analysis of estrogen receptor (ER)-negative, progesterone receptor (PR)-negative, and HER2-negative invasive breast cancer, the so-called triple-negative phenotype: a population-based study from the California Cancer Registry. *Cancer* 2007; **109**: 1721–8.
7 Goldhirsch A, Ingle JN, Gelber RD *et al.* Thresholds for therapies: highlights of the St Gallen international expert consensus on the primary therapy of early breast cancer 2009. *Ann Oncol* 2009; **20**: 1319–29.
8 Luck AA, Evans AJ, James JJ *et al.* Breast carcinoma with basal phenotype: mammographic findings. *AJR Am J Roentgenol* 2008; **191**: 346–51.
9 Tamaki K, Sasano H, Ishida T *et al.* Comparison of core needle biopsy (CNB) and surgical specimens for accurate preoperative evaluation of ER, PgR and HER2 status of breast cancer patients. *Cancer Sci* 2010; **101**: 2074–9.
10 D'Orsi CJ, Bassett LW, Berg WA *et al. Breast Imaging Reporting and Data System: ACR BI-RADS-Mammography*, 4th edn. Reston, Virginia: American College of Radiology, 2003.
11 Tavassoli FA, Devilee P. *World Health Organization Classification of Tumors. Tumor of the Breast and Females Gentia Organs*. Lyon: IARC Press, 2003.
12 Rosen PP. *Rosen's Breast Pathology*, 3rd edn. Philadelphia: Lippincott Williams & Wilkins, 2009.
13 Allred DC, Harvey JM, Berardo M, Clark GM. Prognostic and predictive factors in breast cancer by immunohistochemical analysis. *Mod Pathol* 1998; **11**: 155–68.
14 Wolff AC, Hammond MH, Schwartz JN *et al.* American Society of Clinical Oncology/College of American Pathologists guideline recommendations for human epidermal growth factor receptor 2 testing in breast cancer. *J Clin Oncol* 2007; **25**: 118–45.
15 Spyratos F, Ferrero-Pous M, Trassard M *et al.* Correlation between MIB-1 and other proliferation marker clinical implications of the MIB-1 cutoff value. *Cancer* 2002; **94**: 2151–9.
16 Goldhirsch A, Wood WC, Coates AS *et al.* Strategies for subtypes-dealing with the diversity of breast cancer: highlights of the St Gallen International Expert Consensus on the Primary Therapy of Early Breast Cancer 2011. *Ann Oncol* 2011; **22**: 1736–47.
17 Taneja S, Evans AJ, Rakha EA *et al.* The mammographic correlations of a new immunohistochemical classification of invasive breast cancer. *Clin Radiol* 2008; **63**: 1228–35.
18 Jalava P, Kuopio T, Juntti-Patinen L *et al.* Ki67 immunohistochemistry: a valuable marker in prognostication but with a risk of misclassification: proliferation subgroups formed based on Ki67 immunoreactivity and standardized mitotic index. *Histopathology* 2006; **48**: 674–82.
19 Tabar L, Tony Chen HH, Amy Yen MF *et al.* Mammographic tumor features can predict long-term outcomes reliably in women with 1–14-mm invasive breast carcinoma. *Cancer* 2004; **101**: 1745–59.
20 Evan AJ, Pinder SE, James JJ *et al.* Is mammographic spiculation an independent, good prognostic factor in screening detected invasive breast cancer? *AJR Am J Roentgenol* 2006; **187**: 1377–80.
21 Ko ES, Lee BH, Kim HA *et al.* Triple-negative breast cancer: correlation between imaging and pathological findings. *Eur Radiol* 2010; **20**: 1111–7.
22 Doyle S, Evans AJ, Rakha EA *et al.* Influence of E-cadherin expression on the mammographic appearance of invasive nonlobular breat carcinoma detected at screening. *Radiology* 2009; **253**: 51–5.
23 Gastl G, Spizzo G, Obrist P *et al.* Ep-CAM overexpression in breast cancer as a predictor of survival. *Lancet* 2000; **356**: 1981–2.

© 2011 Japanese Cancer Association

Intracytoplasmic Lipid Accumulation in Apocrine Carcinoma of the Breast Evaluated With Adipophilin Immunoreactivity: A Possible Link Between Apocrine Carcinoma and Lipid-rich Carcinoma

Suzuko Moritani, MD, Shu Ichihara, MD,* Masaki Hasegawa, MD,* Tokiko Endo, MD,† Mikinao Oiwa, MD,† Misaki Shiraiwa, MD,† Chikako Nishida, MD,† Takako Morita, MD,† Yasuyuki Sato, MD,‡ Takako Hayashi, MD,‡ and Aya Kato, MD‡*

Abstract: Although apocrine carcinoma is a distinct histologic entity, there is no immunohistochemical marker to confirm apocrine differentiation with high sensitivity and specificity, and its differential cytologic characteristics are still not fully clarified. Despite the foamy cytoplasm of some apocrine carcinomas and the existence of lipid in the normal apocrine gland, intracytoplasmic lipid in apocrine carcinomas has not been fully explored. By using immunohistochemistry for adipophilin, which is a specific marker of lipid accumulation that can be applied to paraffin sections, we examined intracytoplasmic lipid in apocrine carcinomas. Twenty-four of 26 (92%) apocrine carcinomas and 38 of 116 (33%) nonapocrine carcinomas contained intracytoplasmic lipid. The frequency of adipophilin-positive cases was significantly higher in apocrine carcinomas compared with nonapocrine carcinomas ($P < 0.01$). The positive cell rate per tumor ranged from 10% to 70% (mean, 29%) for apocrine carcinomas. The staining density was heterogeneous from cell to cell. There was no difference in the staining pattern of adipophilin between apocrine ductal carcinoma in situ and invasive apocrine carcinoma or between eosinophilic cells and foamy cells. Sporadic or mosaic distribution of adipophilin-positive cells throughout the tumor and microvesicular or fine granular cytoplasmic staining with heterogeneous density were characteristic features of apocrine carcinoma. Although intracytoplasmic lipid was identified in most apocrine carcinomas, none of the apocrine carcinomas contained prominent intracytoplasmic lipid in >90% of the tumor cells; thus, the criteria for lipid-rich carcinoma was not fulfilled. However, the immunohistochemical study suggests that lipid-rich carcinomas are closely related to apocrine carcinomas.

From the *Department of Advanced Diagnosis, Division of Pathology; †Department of Advanced Diagnosis, Laboratory of Imaging Diagnosis; and ‡Department of Surgery, Nagoya Medical Center, Sannomaru, Naka-ku, Nagoya, Aichi, Japan.

Supported by a Grant-in-Aid for clinical research from the National Hospital Organization of Japan.

Correspondence: Suzuko Moritani, MD, Department of Advanced Diagnosis, Division of Pathology, Nagoya Medical Center, 4-1-1 Sannomaru, Naka-ku, Nagoya, Aichi 460-0001, Japan (e-mail: MoritaniS@aol.com).

Copyright © 2011 by Lippincott Williams & Wilkins

Key Words: apocrine carcinoma, intracytoplasmic lipid, lipid-rich carcinoma, adipophilin, paraffin sections

(*Am J Surg Pathol* 2011;35:861–867)

Apocrine carcinoma of the breast is defined as a carcinoma showing cytologic and immunohistochemical features of apocrine cells in >90% of the tumor cells.[22] The cytologic features of apocrine differentiation are abundant eosinophilic granular or foamy cytoplasm and a large nucleus with prominent nucleolus. Apocrine carcinomas are immunohistochemically characterized as estrogen receptor negative, progesterone receptor negative, bcl-2 negative, androgen receptor (AR) positive, and gross cystic disease fluid protein 15 (GCDFP-15) positive.[2,5,9,10,12,19,20] The diagnosis of typical apocrine carcinoma is usually straightforward; however, the histologic recognition of sebocrine and histiocytoid variants of apocrine carcinoma is occasionally subjective. There is no commercially available and stable immunohistochemical marker that is both sensitive and specific to apocrine differentiation. The reported frequency of apocrine carcinoma is variable depending on the definition of apocrine carcinoma that is used. On the basis of the findings of hematoxylin and eosin (HE)-stained sections, the frequency is 0.3% to 4%.[16] On the basis of the GCDFP-15 staining pattern, the frequency is 12% to 72%.[5,16] This variability reflects the discrepancy between apocrine carcinoma defined by histologic criteria and apocrine carcinoma defined by the apocrine markers that are present. Thus, unique cytologic features of apocrine carcinoma that differentiate it from other breast carcinomas with similar cytologic features are still not fully characterized.

The histology of the normal apocrine gland is characterized by luminal cells composed of eosinophilic cytoplasm, which may contain lipid, iron, lipofuscin, glycogen granules, and a large nucleus located near the base of the cell.[13] We focused on the relationships between intracytoplasmic lipid in the normal apocrine gland and in the foamy cytoplasm of some apocrine carcinomas. Although the foamy cytoplasm reminds us of the presence

of lipid, intracytoplasmic lipid in apocrine carcinoma has not been extensively examined. The histochemical staining of intracytoplasmic lipid requires frozen sections, which are not always available for routine surgical cases. Recently, several immunohistochemical markers that recognize lipid accumulation on paraffin sections became commercially available.[15] Of these markers, adipophilin was identified in normal lactating breast lobules and sebaceous carcinomas of the breast.[8,14] In this study, we used adipophilin immunohistochemistry to determine whether intracytoplasmic lipid is a common feature of apocrine carcinoma.

MATERIALS AND METHODS

Twenty-six apocrine carcinomas were retrieved from the surgical pathology files of the Nagoya Medical Center between 2003 and 2008. A total of 1058 breast surgeries were performed during this period. We selected only unequivocal cases of apocrine carcinoma by strictly following the morphologic criteria of the 2003 World Health Organization classification system.[22] At least 2 pathologists who are subspecialists in breast pathology (S.M. and S.I.) confirmed the diagnosis of apocrine carcinoma. The control group consisted of 116 consecutive nonapocrine breast cancers that were surgically resected between March and December 2009. Cases in which chemotherapy, hormonal therapy, or radiation was performed before the surgery were excluded. We also included 2 cases of lipid-rich carcinoma.

Of the 26 apocrine carcinomas, 15 were ductal carcinoma in situ (DCIS) and 11 were invasive apocrine carcinoma. Of the 15 apocrine DCIS, 12 were high grade and 3 were intermediate grade. All 11 invasive apocrine carcinomas were grade 3 according to the modified Scarff-Bloom-Richardson classification system.[4] The 116 nonapocrine controls consisted of 59 invasive ductal carcinomas, not otherwise specified (IDC, NOS); 25 DCIS; 10 invasive lobular carcinomas (ILCs); 6 invasive micropapillary carcinomas (IMPCs); 3 mixed IMPC and IDC, NOS (IMPC and IDC); 3 mucinous carcinomas (Mucs); 2 mixed Mucs and IDC, NOS (Muc and IDC); 4 solid neuroendocrine carcinomas (SNs); 2 solid papillary carcinomas; 1 adenoid cystic carcinoma; and 1 tubular carcinoma. One of the 2 cases of lipid-rich carcinoma was retrieved from the consultation files of S.I. The other was an already published case of lipid-rich carcinoma that was contributed to us by the researcher.[24]

After histopathologic evaluation, representative slides of the lesions were selected for immunohistochemical examination of adipophilin, GCDFP-15, and AR. The slides were heated in a citrate buffer (pH 6.0) at 121°C for 15 minutes, except in the case of GCDFP-15 immunohistochemistry. The following primary antibodies were used: a 1:50 dilution of anti-adipophilin (clone AP125; Acris Antibodies GmbH, Hiddenhausen, Germany); a 1:50 dilution of anti-AR (clone AR441; Dako Cytomation, Glostrup, Denmark); and prediluted anti-GCDFP-15 (clone D6; Signet, Dedham, MA). Signals were detected by using the Dako REAL EnVision detection system and Peroxidase/DAB+ (Dako Cytomation), according to the instructions of the manufacturer.

The percentage of tumor cells that were positive for adipophilin, GCDFP-15, and AR was evaluated semiquantitatively by gross inspection. Tumor specimens were considered positive for a marker if the marker expression was found in $>10\%$ of the tumor cells. This cutoff level was arbitrarily determined.

The χ^2 test was used for statistical analyses, and P values <0.01 were considered to be statistically significant.

RESULTS

The results of immunohistochemistry are summarized in Table 1. Twenty-four of 26 (92%) apocrine carcinomas were adipophilin positive. These adipophilin-positive tumors consisted of 14 of the 15 apocrine DCIS and 10 of the 11 invasive apocrine carcinomas. The signals were located in the cytoplasm and had a microvesicular or fine granular pattern (Figs. 1A–D). The positive cell rate within tumors ranged from 10% to 70%. Eighteen of 24 (75%) adipophilin-positive apocrine carcinomas had positive signals in $<50\%$ of the tumor cells, and the other 6 adipophilin-positive apocrine carcinomas (25%) had positive signals in 50% or more of the tumor cells. The average positive cell rate within 1 tumor was 29%. The staining density of each tumor cell was variable from cell to cell. The distribution pattern in positive cells was sporadic or diffuse throughout the tumor, and a focal pattern was rare. Not only foamy cells but also eosinophilic granular cells were positive for adipophilin, and there was no visible difference in the positive cell rate and staining density between

TABLE 1. Immunohistochemistry Results

	Adipophilin	AR	GCDFP-15
Apocrine carcinoma (n = 26)	24 (92%)	25 (96%)	24 (92%)
DCIS (n = 15)	14 (93%)	14 (93%)	13 (87%)
Invasive (n = 11)	11 (91%)	11 (100%)	11 (100%)
Nonapocrine carcinoma (n = 116)	38 (33%)	71 (61%)	41 (35%)
DCIS (n = 25)	9 (36%)	19 (76%)	12 (48%)
IDC, NOS (n = 59)	23 (39%)	36 (61%)	22 (37%)
ILC (n = 10)	5 (50%)	7 (70%)	2 (20%)
IMPC (n = 6)	0	4 (67%)	0
IMPC+IDC (n = 3)	0	1 (33%)	0
Muc (n = 3)	0	2 (67%)	2 (67%)
Muc+IDC (n = 2)	0	1 (50%)	0
SN (n = 4)	0	1 (25%)	1 (25%)
SPC (n = 2)	0	0	2 (100%)
ACC (n = 1)	1 (100%)	0	0
Tub (n = 1)	0	0	0
Lipid-rich carcinoma (n = 2)	2 (100%)	0	2 (100%)

ACC indicates adenoid cystic carcinoma; IMPC+IDC, mixed invasive micropapillary and invasive ductal carcinoma; Muc+IDC, mixed mucinous and invasive ductal carcinoma; SPC, solid papillary carcinoma.

© 2011 Lippincott Williams & Wilkins

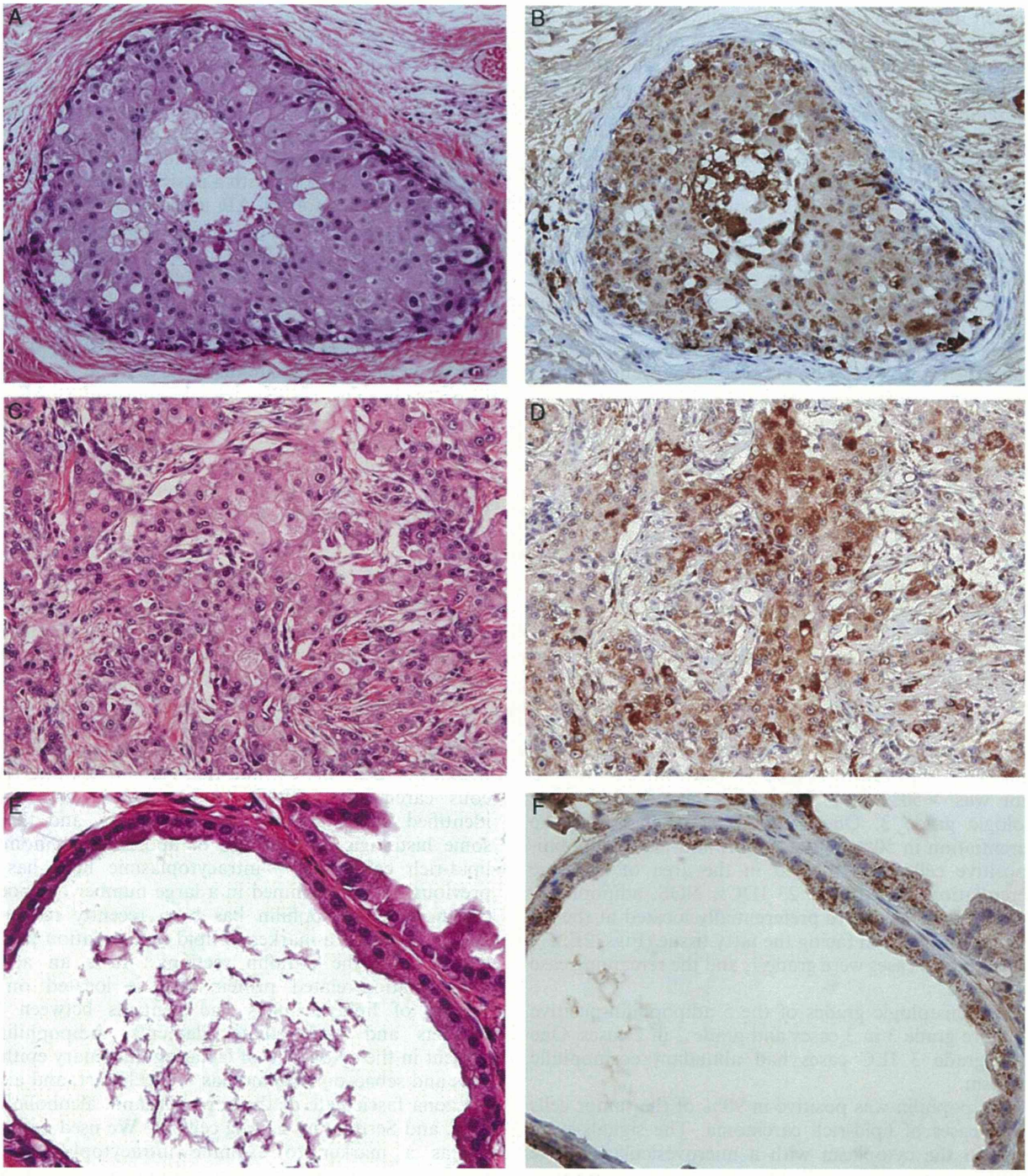

FIGURE 1. Adipophilin expression in apocrine carcinomas and benign apocrine gland. The signals present in the cytoplasm with a microvesicular or fine granular pattern. A and B, Apocrine DCIS. In addition to the tumor cells, clusters of foamy macrophages at the center were diffusely positive. C and D, Invasive apocrine carcinoma. E and F, Benign apocrine gland.

eosinophilic granular cells and foamy cells. There was no difference in the staining pattern and positive cell rate between apocrine DCIS and invasive apocrine carcinomas. All 15 apocrine DCIS contained clusters of foamy macrophages at the center of the ductal lumen that was affected by cancer, and these foamy macrophages were strongly positive for adipophilin. Great care was taken not to confuse non-neoplastic adipophilin-positive cells with adipophilin-positive tumor cells. For example, clusters of adipophilin-positive foamy macrophages were

© 2011 Lippincott Williams & Wilkins

also seen in areas in which tumor cells were negative for adipophilin. Non-neoplastic apocrine cysts were also present in the background in some cases, and the non-neoplastic apocrine epithelia were also positive for adipophilin with a microvesicular or fine granular pattern (Figs. 1E, F).

Thirty-eight of the 116 (33%) nonapocrine carcinomas were adipophilin positive. The 38 cases consisted of 23 of the 59 (39%) IDCs, NOS, 9 of the 25 (36%) DCISs, 5 of the 10 (50%) ILCs, and 1 adenoid cystic carcinoma. The positive cell rate within the tumors ranged from 10% to 90%, and the average positive cell rate was 30%. The frequency of adipophilin-positive cases was significantly higher in apocrine carcinomas than in nonapocrine carcinomas ($P < 0.01$). However, there was no difference in the average positive cell rate between adipophilin-positive apocrine and nonapocrine carcinomas.

Among the 9 cases of adipophilin-positive nonapocrine DCISs, the histologic grade was high in 3 cases, intermediate in 3 cases, and low in 3 cases. The positive cell rate within each tumor was < 30% in 8 of the 9 cases. However, 1 high-grade DCIS associated with Paget disease was diffusely positive for adipophilin in 80% of the tumor. In 8 of 9 DCISs, adipophilin-positive tumor cells tended to have foamy or eosinophilic granular cytoplasm, and clusters of foamy macrophages were seen in 5 of these cases (Figs. 2A, B).

Among the 23 cases of adipophilin-positive nonapocrine IDC, NOS, the histologic grade was grade 3 in 8 cases, grade 2 in 8 cases, and grade 1 in 7 cases. In 11 of the 23 (48%) IDCs, NOS, the adipophilin-positive tumor cells had abundant foamy or eosinophilic granular cytoplasm (Figs. 2C, D). The positive cell rate within each tumor was > 50% in 5 cases, and these 5 cases were histologic grade 3. One of these cases had apocrine differentiation in 50% of the tumor, and most adipophilin-positive cells were located in the area of apocrine differentiation. In 5 of the 23 IDCs, NOS, adipophilin-positive tumor cells were preferentially located at the tip of the tumor invasion facing the fatty tissue (Figs. 2E, F). Four of these 5 cases were grade 1, and the remaining case was grade 2.

The histologic grades of the 5 adipophilin-positive ILCs were grade 3 in 3 cases and grade 2 in 2 cases. One of the grade 3 ILC cases had abundant eosinophilic cytoplasm.

Adipophilin was positive in 90% of the tumor cells in both cases of lipid-rich carcinoma. The signals were present in the cytoplasm with a microvesicular or fine granular pattern (Figs. 2G, H). The signal intensity in individual tumor cells was heterogeneous.

Twenty-five of the 26 (96%) apocrine carcinomas and 71 of the 116 (61%) nonapocrine carcinomas were AR positive. Both lipid-rich carcinomas were AR negative. The frequency of AR-positive cases was significantly higher in apocrine carcinomas than in nonapocrine carcinomas ($P < 0.01$). The average AR-positive cell rate within each tumor was 43% for apocrine carcinomas and 62% for nonapocrine carcinomas. GCDFP-15 was positive in 24 of the 26 (92%) apocrine carcinomas and 41 of the 116 (35%) nonapocrine carcinomas. The frequency of GCDFP-15-positive cases was significantly higher in apocrine carcinomas than in nonapocrine carcinomas ($P < 0.01$). The average GCDFP-15 positive cell rate per tumor was 51% in apocrine carcinomas and 32% in nonapocrine carcinomas. Both lipid-rich carcinomas were positive for GCDFP-15 with a positive cell rate of 20% or 30%. The expression of AR and GCDFP-15 in adipophilin-positive carcinomas is summarized in Table 2. Twenty-one of 26 (81%) apocrine carcinomas were positive for all 3 markers (adipophilin, AR, and GCDFP-15), whereas only 12 of 116 (10.3%) nonapocrine carcinomas were positive for all 3 markers. The sensitivities of adipophilin, AR, and GCDFP-15 as a marker of apocrine carcinoma were 92%, 96%, and 92%, respectively. The specificities of adipophilin, AR, and GCDFP-15 as a marker of apocrine carcinoma were 68%, 40%, and 65%, respectively. If the 3 markers were used in combination, and apocrine differentiation was defined as positivity of all 3 markers, the sensitivity was 88% and the specificity was 90%.

DISCUSSION

Various amounts of intracytoplasmic lipid were seen in 75% of breast carcinomas, as determined by histochemical staining of frozen sections.[6] However, there are limited data on this issue, probably due to the technical difficulty of lipid staining in routine surgical specimens. The detailed histologic features of lipid-containing breast carcinomas were not previously known, with the exceptions of lipid-rich carcinomas and sebaceous carcinomas. Although intracytoplasmic lipid is identified in the normal apocrine gland, and there is some histologic resemblance of apocrine carcinoma to lipid-rich carcinoma,[23] intracytoplasmic lipid has not previously been examined in a large number of apocrine carcinomas. Adipophilin has been recently recognized and validated as a marker of lipid accumulation that can be used on the paraffin sections.[8] It is an adipose differentiation-related protein that is located on the surface of lipid droplets and contacts between lipid droplets and intermediate filaments. Adipophilin is present in the cytoplasm of lactating mammary epithelial cells and sebaceous carcinomas of the breast, and also in the zona fasciculate of the adrenal gland, alcoholic fatty liver, and Sertoli and Leydig cells.[8,14] We used adipophilin as a marker to examine intracytoplasmic lipid accumulation in 26 apocrine carcinomas, 116 nonapocrine control carcinomas, and 2 lipid-rich carcinomas. This is the first report of the intracytoplasmic lipid status of a large number of breast carcinomas evaluated by paraffin sections.

With an arbitrarily determined cutoff index of 10%, there was a significant difference in adipophilin expression between apocrine and nonapocrine carcinomas. The tumor cells of apocrine carcinomas contained various amounts of intracytoplasmic lipid significantly more

© 2011 Lippincott Williams & Wilkins

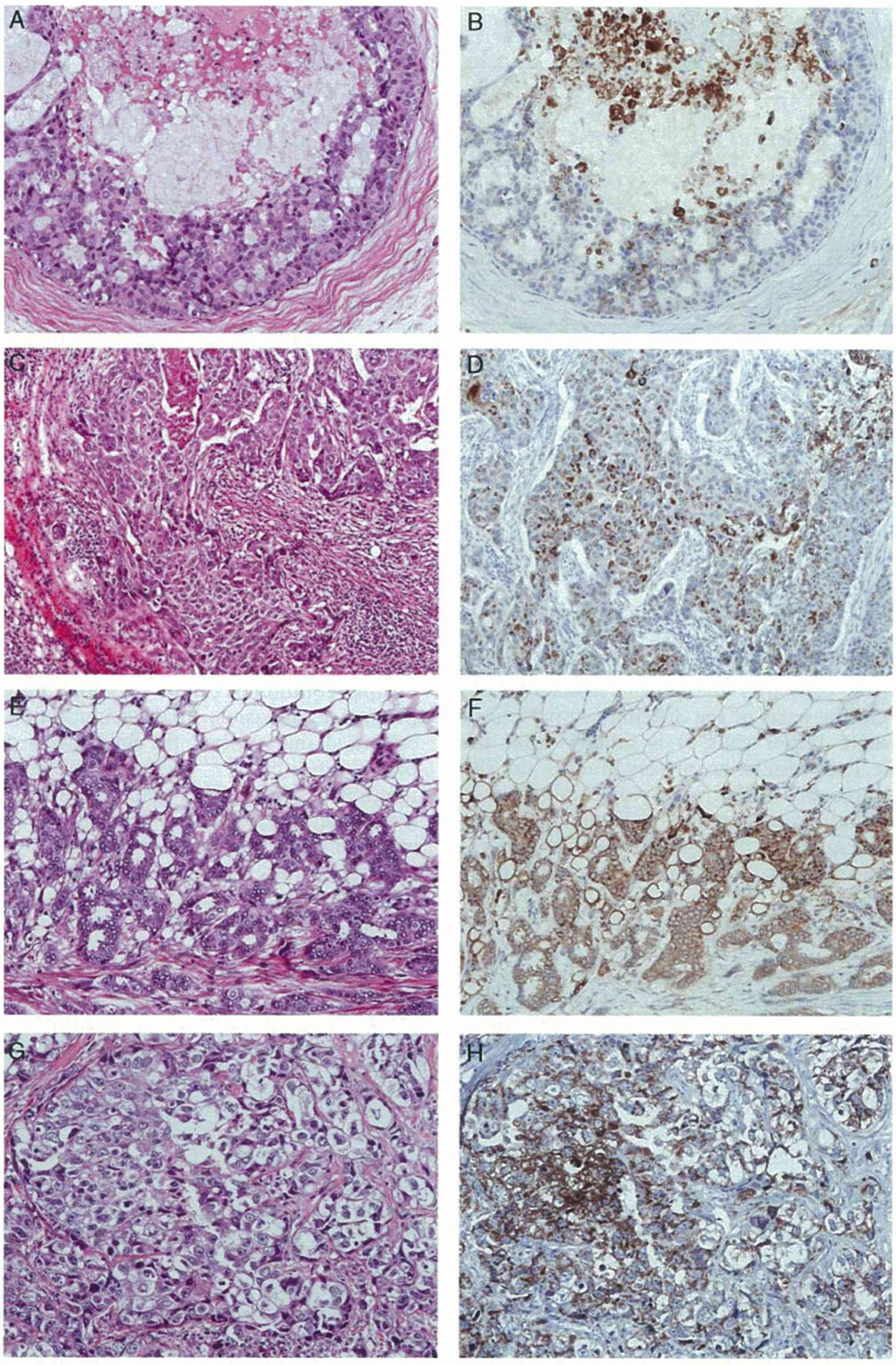

FIGURE 2. Adipophilin expression in nonapocrine carcinomas. A and B, DCIS. The adipophilin-positive tumor cells tended to have abundant eosinophilic or foamy cytoplasm. Clusters of foamy macrophages were also positive. C and D, IDC, NOS, grade 3. E and F, IDC, NOS, grade 1. In this case, adipophilin-positive tumor cells were preferentially located at the tip of the tumor invasion facing the fatty tissue. G and H, Lipid-rich carcinoma. Most of the tumor cells were positive with heterogeneous signal intensity.

© *2011 Lippincott Williams & Wilkins*

TABLE 2. Expression of AR and GCDFP-15 in Adipophilin-Positive Carcinomas

	AR	GCDFP-15	Both
Apocrine carcinoma (n = 24)	23 (96%)	23 (96%)	21 (88%)
Nonapocrine carcinoma (n = 38)	23 (61%)	17 (45%)	12 (32%)
DCIS (n = 9)	6 (67%)	4 (44%)	4 (44%)
IDC, NOS (n = 23)	14 (61%)	11 (48%)	7 (30%)
ILC (n = 5)	3 (60%)	2 (40%)	1 (20%)
ACC (n = 1)	0	0	0
Lipid-rich carcinoma (n = 2)	0	2 (100%)	0

ACC indicates adenoid cystic carcinoma; Both, adipophilin-positive carcinoma that was positive for both AR and GCDFP-15.

frequently than nonapocrine carcinomas. Our results suggest that intracytoplasmic lipid is one of the common cytologic characteristics of apocrine carcinomas. The presence of intracytoplasmic lipid may reflect the functional differentiation of lipid secretion just like normal apocrine gland epithelial cells. The presence of adipophilin-positive luminal foam cells in all 15 cases of apocrine DCIS also supports this hypothesis. Damiani et al[3] reported that luminal foam cells could be either histiocytic or foamy apocrine cells. The presence of lipid in these foam cells reflects lipid secretion from the neoplastic apocrine epithelial cells and the phagocytosis of lipid by histiocytes. On the basis of the distribution pattern of adipophilin-positive tumor cells, it is unlikely that the intracytoplasmic lipid would be present due to the degeneration phenomenon. If the intracytoplasmic lipid in apocrine carcinomas accumulated as a result of cellular damage caused by ischemia, it should be distributed preferentially near the necrotic foci or the areas remote to the blood vessels.

It should be noted that 20 of 38 (53%) adipophilin-positive nonapocrine carcinomas had foamy and/or eosinophilic cytoplasm at least focally, and such cells tended to be adipophilin positive. In addition, 12 of 38 (32%) adipophilin-positive nonapocrine carcinomas were positive for both AR and GCDFP-15. We selected the apocrine carcinomas with strict morphologic criteria. We required the presence of typical apocrine features in both the cytoplasm and nuclei, and we did not refer to the results of immunohistochemistry to make our determination. It is possible that adipophilin-positive areas of some nonapocrine carcinomas might reflect focal apocrine differentiation or incomplete apocrine differentiation.

Another interesting observation was the tendency of adipophilin-positive cells in 5 nonapocrine carcinomas to be located at the tips of tumors invading fatty tissue. All 5 tumors showing such a staining pattern were nonhigh-grade IDC, NOS without notable histologic features. The significance of this localization is unclear, but there is a possibility of passive lipid accumulation due to the interaction between tumor cells and surrounding fat cells.

We also evaluated the usefulness of adipophilin, compared with AR and GCDFP-15, as a marker of apocrine carcinomas. The sensitivity and specificity of adipophilin were almost the same as those of GCDFP-15. With respect to specificity, adipophilin seems to be a better marker of apocrine carcinoma than AR. However, in 75% of adipophilin-positive apocrine carcinomas, the positive cell rate per tumor was < 50%, and the average positive cell rate was 29%. The density of positive signals in individual tumor cells was variable, and the positive signals were rarely diffusely and strongly positive. We consider adipophilin to be a useful marker of apocrine carcinoma; however, its usefulness for small needle biopsy specimens might be limited. When AR, DCDFP-15, and adipophilin were used in combination, and positivity for all 3 markers was used as an apocrine marker, the specificity increased to 90%. Adipophilin is a useful marker of apocrine carcinoma when it is used in combination with AR and GCDFP-15.

An important differential diagnosis of apocrine carcinoma is lipid-rich carcinoma, a very rare histologic type of breast carcinoma in which approximately 90% of tumor cells contain abundant cytoplasmic neutral lipid. Conventional HE sections of lipid-rich carcinomas contain tumor cells with vacuolated, foamy, or clear cytoplasm.[1,17] Ultrastructurally, the cytoplasm is rich in rough endoplasmic reticulum with prominent Golgi apparatus, and lipid vesicles are located near the Golgi apparatus.[17] These ultrastructural findings and the homogenous distribution of lipid-containing tumor cells with mitosis indicate that the intracytoplasmic lipid accumulation is not a degenerative change; rather, the lipids are a secretory product of the tumor cells.[1,17] As the morphology on HE sections resembles glycogen-rich clear cell carcinoma and apocrine carcinoma, the definitive diagnosis of lipid-rich carcinoma is difficult without histochemical staining or ultrastructural study. Glycogen-rich clear cell carcinoma can be differentiated from lipid-rich carcinoma with periodic acid-Schiff staining with diastase treatment.[7] The differential diagnosis between apocrine carcinoma and lipid-rich carcinoma has not been extensively evaluated, although 1 study commented on the lack of intracytoplasmic lipid in apocrine carcinoma.[18] In this study, we found that intracytoplasmic lipid is common in apocrine carcinomas; however, the positive cell rate per tumor ranged from 10% to 70%, and the average positive cell rate per 1 tumor was only 29%. Furthermore, the staining density in individual tumor cells was not homogenously strong. In contrast, the 2 lipid-rich carcinomas showed diffuse positivity for adipophilin in approximately 90% of tumor cells with heterogeneous signal density. Although it is a very limited number of cases, the positive cell rate was apparently higher in lipid-rich carcinomas than in apocrine carcinomas. We consider sporadic and heterogeneous staining patterns to be a characteristic feature of apocrine carcinoma that distinguishes it from lipid-rich carcinoma. The difference between apocrine carcinomas and lipid-rich carcinomas might only be the difference in the percentage of lipid-containing tumor cells. It is notable that the 2 lipid-rich carcinomas in this study showed focal positivity for GCDFP-15. In addition, the relatively high nuclear grade and hormone receptor

© 2011 Lippincott Williams & Wilkins

negativity of lipid-rich carcinomas shown by a limited number of studies partly support the close resemblance of the 2 entities.[21,22] Lipid-rich carcinoma might not be a distinct histologic entity, but at least some lipid-rich carcinomas might be a subtype of apocrine carcinomas that are extremely rich in cytoplasmic lipid. An immunohistochemical study of intracytoplasmic lipid accumulation in paraffin sections from a large number of lipid-rich carcinomas and a comparison of the immunohistochemical profile (including adipophilin, hormone receptors, GCDFP-15, and bcl-2) with apocrine carcinomas would be necessary to confirm this hypothesis.

The clinical significance of intracytoplasmic lipid in breast cancer has been hardly addressed, with the exception of one study by Fisher et al[6] more than 3 decades ago. They examined intracytoplasmic lipid in 87 consecutive surgical cases of breast cancer by using oil red O, and they found a positive correlation between lipid content with high histologic grade and short-term treatment failure. Sporadic case reports and clinicopathologic analyses of a small number of lipid-rich carcinomas, many of which were from before the era of modern chemotherapy, suggest aggressive clinical behavior.[1,11,17] In contrast, the prognosis of apocrine carcinoma is considered to be not significantly different from that of nonapocrine carcinoma.[22,23] However, the number of lipid-rich carcinoma cases reported to date is extremely small compared with apocrine carcinoma. The rarity of lipid-rich carcinoma might be at least partly due to the technical difficulty of identifying lipid on routine histologic sections. The ability to perform immunohistocmehistry for adipophilin with paraffin sections made it easier for us to identify intracytoplasmic lipid in large number of cases and will enable us to identify more cases of lipid-rich carcinomas. This new method will allow for a reappraisal of lipid-rich carcinomas that will clarify the clinical significance of intracytoplasmic lipid in breast cancer.

ACKNOWLEDGMENT

The authors are grateful to Dr Airo Tsubura, Dr Kenzo Ono, and Dr Masato Nakaguro for kindly providing the cases of lipid-rich carcinoma.

REFERENCES

1. Aboumrad MH, Horn RC, Fine G. Lipid-secreting mammary carcinoma. *Cancer*. 1963;16:521–525.
2. Celis JE, Cabezón T, Moreira JMA, et al. Molecular characterization of apocrine carcinoma of the breast: validation of an apocrine protein signature in a well-defined cohort. *Mol Oncol*. 2009;3:220–237.
3. Damiani S, Cattani MG, Buonamici L, et al. Mammary foam cells: characterization by immunohistochemistry and in situ hybridization. *Virchows Arch*. 1998;432:433–440.
4. Elston CW, Ellis IO. Pathological prognostic factors in breast cancer I. The value of histological grade in breast cancer: experience from a large study with long follow up. *Histopathology*. 1991;19:403–410.
5. Eusebi V, Millis RR, Cattani MG, et al. Apocrine carcinoma of the breast: a morphologic and immunocytochemical study. *Am J Pathol*. 1986;123:532–541.
6. Fisher ER, Gregorio R, Kim WS, et al. Lipid in invasive cancer of breast. *Am J Clin Pathol*. 1977;68:558–561.
7. Hayes MMM, Seidman JD, Ashton MA. Glycogen-rich clear cell carcinoma of the breast: a clinicopathologic study of 21 cases. *Am J Surg Pathol*. 1995;19:904–911.
8. Heid HW, Moll R, Schwetlick I, et al. Adipophilin is a specific marker of lipid accumulation in diverse cell types and diseases. *Cell Tissue Res*. 1998;294:309–321.
9. Honma N, Takubo K, Akiyama F, et al. Expression of GCDFP-15 and AR decreases in larger or node-positive apocrine carcinomas of the breast. *Histopathology*. 2005;47:195–201.
10. Honma N, Takubo K, Akiyama F, et al. Expression of oestrogen receptor-β in apocrine carcinoma of the breast. *Histopathology*. 2007;50:425–433.
11. Kurebayashi J, Izuo M, Ishida T, et al. Two cases of lipid-secreting carcinoma of the breast: case reports with an electron microscopic study. *Jpn J Clin Oncol*. 1988;18:249–254.
12. Leal C, Henrique R, Monteiro P, et al. Apocrine ductal carcinoma in situ of the breast: histologic classification and expression of biologic markers. *Hum Pathol*. 2001;32:487–493.
13. Li M, Urmacher CD. Normal skin. In: Mills SE, ed. *Histology for Pathologists*. Philadelphia, PA: Lippincott Williams & Wilkins; 2007:3–28.
14. Murakami A, Kawachi K, Sasaki T, et al. Sebaceous carcinoma of the breast. *Pathol Int*. 2009;59:188–192.
15. Muthusamy K, Halbert G, Roberts F. Immunohistochemical staining for adipophilin, perilipin and TIP47. *J Clin Pathol*. 2006;59:1166–1170.
16. O'Malley FPO, Bane AL. The spectrum of apocrine lesions of the breast. *Adv Anat Pathol*. 2004;11:1–9.
17. Ramos CV, Taylor HB. Lipid-rich carcinoma of the breast: a clinicopathological analysis of 13 examples. *Cancer*. 1974;33:812–819.
18. Reis-Filho JS, Fulford LG, Lakhani SR, et al. Pathology quiz case: a 62-year-old woman with a 4.5-cm nodule in the right breast. *Arch Pathol Lab Med*. 2003;127:e396–e398.
19. Sapp M, Malik A, Hanna W. Hormone receptor profile of apocrine lesions of the breast. *Breast J*. 2003;9:335–336.
20. Selim AGA, El-Ayat G, Wells CA. Androgen receptor expression in ductal carcinoma in situ of the breast: relation to oestrogen and progesterone receptors. *J Clin Pathol*. 2002;55:14–16.
21. Shi P, Wang M, Zhang Q, et al. Lipid-rich carcinoma of the breast: a clinicopathological study of 49 cases. *Tumori*. 2008;94:342–346.
22. Tavassoli FA, Devilee P, eds. *World Health Organization Classification of Tumors. Pathology and Genetics of Tumors of the Breast and Female Genital Organs*. Lyon: IARC Press.
23. Tavassoli FA, Eusebi V, eds. *AFIP Atlas of Tumor Pathology, Series 4, Tumors of the Mammary Gland*. Washington DC: American Registry of Pathology; 2009.
24. Tsubura A, Hatano T, Murata A, et al. Breast carcinoma in patients receiving neuroleptic therapy: morphologic and clinicopathologic features of thirteen cases. *Acta Pathol Jpn*. 1992;42:494–499.

© 2011 Lippincott Williams & Wilkins

原　著

新規開発直接変換型ディジタルマンモグラフィ装置の最適な撮影条件の検討

遠藤登喜子[1,2]・白岩美咲[1,2]・大岩幹直[1,2]・西田千嘉子[1,2]
森田孝子[1,2]・吉川和明[1,3]・佐藤康幸[4]・林　孝子[4]
市原　周[1,5]・森谷鈴子[1,5]・広藤喜章[1,2]・若山卓也[1,2]

1)国立病院機構名古屋医療センター高度診断研究部
2)国立病院機構名古屋医療センター放射線科
3)財団法人島根県環境保健公社
4)国立病院機構名古屋医療センター外科
5)国立病院機構名古屋医療センター研究検査科病理

論文受付
2010年 8 月26日
論文受理
2011年 7 月13日
Code No. 230

緒　言

マンモグラフィはアナログ式のscreen-film方式から始まった．アナログ式は適切な撮影を行えば非常に鮮明な画像が得られるが，X線を信号に変える効率detective quantum efficiency(DQE)が低いため，厚みのある乳房には向かないというデメリットがあった．マンモグラフィ装置のディジタル化は，computed radiography(CR)やfull field digital mammogaphy

Optimization of Exposure Conditions for Amorphous Selenium Direct Conversion DR-based Mammography System

Tokiko Endo,[1,2] Misaki Shiraiwa,[1,2] Mikinao Oiwa,[1,2] Chikako Nishida,[1,2] Takako Morita,[1,2] Kazuaki Yoshikawa,[1,3] Yasuyuki Sato,[4] Takako Hayashi,[4] Shu Ichihara,[1,5] Suzuko Moritani,[1,5] Yoshiaki Hirofuji,[1,2] and Takuya Wakayama[1,2]

1) Department of Advanced Diagnosis, Clinical Research Center, National Hospital Organization Nagoya Medical Center
2) Department of Radiology, National Hospital Organization Nagoya Medical Center
3) Shimane Environment & Health Public Corporation
4) Department of Surgery, National Hospital Organization Nagoya Medical Center
5) Department of Pathology, National Hospital Organization Nagoya Medical Center

Received August 26, 2010; Revision accepted July 13, 2011; Code No. 230

Summary

A new direct-conversion detector for DR mammography has improved the detectability of microcalcifications and masses. Each optimized exposure condition (target/filter combination and tube voltage) was defined through comparison of physical values and visual evaluation on breast specimens using the innovative DR mammography. The contrast-to-noise-ratios (CNRs) of PMMA phantoms of various thicknesses were obtained under a variety of exposure conditions whose average glandular doses (AGDs) were made consistent. Fifty breast specimens were irradiated under these combinations. Visual evaluation was conducted on the images, whose histograms were controlled for consistency. In the phantoms with thicknesses of 20 mm or more, tungsten/rhodium had the highest CNRs of the targets/filters such as molybdenum/molybdenum and molybdenum/rhodium. For visualizing microcalcifications and masses on breast specimens of thicknesses of 35 mm and below, molybdenum/molybdenum was the best. Nevertheless, to obtain better image quality, molybdenum/rhodium was superior for 35–55 mm thickness, and tungsten/rhodium was superior for 55 mm and above under the same AGD, enabling accurate and efficient diagnosis. The study showed that the exposure conditions differ for obtaining the highest CNR using phantoms and those under which breast specimen images allow the most accurate and efficient diagnosis. In addition, image evaluations of the breast specimens allowed optimization of exposure conditions that are closer to those of the actual diagnosis using mammography.

Key words: radiology, mammography, direct conversion, exposure condition, breast cancer

別刷資料請求先：〒460-0001　名古屋市中区三の丸四丁目1番1号
国立病院機構名古屋医療センター高度診断研究部兼同放射線科　遠藤登喜子　宛

(FFDM)のディジタル装置の登場により，2000年の前半に始まった．ディジタル式は現在でも解像度の点ではアナログ式におよばないが，収集したデータに画像処理を加えることで，乳房の特性に合わせての診断に適した画像とすることができる．また，DQEが高いことから，screen-film式に対して同等の画質を得るのに，被ばくを低減できる効果がcontrast-detailファントムを使った研究によって[1,2]，さらに臨床的評価によって示されている[3]．さらに，FFDMはscreen-film式に対してrecall rate(要精検率)が低下する効果が示されている[4]．

FFDMには大別して，間接変換方式と直接変換方式とがある．間接変換方式とは検出器に入射したX線が光に変換された後，電気信号を得る方式である．光は散乱する特性があるため，間接変換方式では鮮鋭度が低くなるディメリットがある．高い鮮鋭度を得るためには，蛍光体の厚みを薄くすればよいが，X線の吸収率を下げることになるため，照射線量を上げなければならない．一方，直接変換方式は，検出器に入射するX線を直接電気信号に変えるため，鮮鋭度が高く，DQEも高い[5]．直接変換方式で用いられるアモルファスセレン(amorphous selenium; a-Se)は，間接変換方式よりも鮮鋭度，およびDQEが高いことが特徴である[5,6]．

以上の特徴をもつFFDMであるが，一方ではsignal-to-noise ratio(SNR)の影響で解像度を上げることが困難である．画素ごとのデータは，一般的にthin film transistor(TFT)を用いて読み出されるが，画素を高密度化するほど電気ノイズが増大する．さらに信号強度は画素面積に比例するため，画素サイズの2乗に比例する．こういったノイズの問題を解決しようとしたのが，直接変換型フラットパネル検出器を搭載した富士フイルム社製AMULETである．この装置はTFTの代わりに，光学式スイッチング方式で信号を読み取るので，従来のTFT方式よりも高いSNRでデータを取得することができる．本研究は，この新しいFFDM装置を対象としている[7]．

X線のエネルギースペクトルは管電圧，ターゲット/フィルタによって決定される線質によって異なり，検出器のX線吸収特性はその材質によって異なる．新しく開発されたディジタルマンモグラフィ装置の使用に際しては，検出器の吸収特性を踏まえ，被写体の厚みに適した線質を選ぶことが必要である．線質を選ぶ方法として，物理評価やファントムでの画質評価を用いる方法が一般的である．これらの方法はかなりの部分が標準化されており，測定者による影響のない客観性の高い情報が得られる．しかし，被写体はファントムであり，実際の被写体とは異なるため，物理評価やファントム評価で決定した撮影条件が実物の乳房撮影に対して最も適しているかの検討が必要であるが，これまで十分に検討された例はなかった．本研究は，物理評価から最適な撮影条件を仮設定した上で，乳房組織を撮影し，その差異を改めて確認しようとするものである．さまざまな条件で乳房組織を撮影し，それらの画像を比較することで撮影条件を設定すれば，臨床画像に基づいた撮影条件の最適化ができる．本研究は，従来行われてきた物理評価とファントム画質評価に加え，乳房組織による評価という新しい手法を提案するものである．また，物理評価に基づき決定した線質が最適なものか，改めて見直そうとするものである．さらに，この新しい手法によって，新規に開発された直接変換型フラットパネル検出器(a-Se)に最適な線質および撮影条件を検討することを目的とした．

1．使用機器および方法

使用装置は富士フイルム株式会社製AMULETで，検出器はa-Seを用い，光学的スイッチング方式により50 μmの画素サイズを実現している[7]．撮影装置に搭載されているターゲット/フィルタはmolybdenum/molybdenum(Mo/Mo)，molybdenum/rhodium(Mo/Rh)，tungsten/rhodium(W/Rh)である．Moフィルタの厚みは30 μmであり，Rhフィルタの厚みはMoターゲットとの組合せで25 μm，Wターゲットとの組合せで50 μmである．

対象装置の画質を示す物理的指標としてcontrast-to-noise ratio(CNR)を用いる方法が提案されており，マンモグラフィ装置間の性能比較[8~10]や日常管理[11]に用いられている．本研究においても，CNRを指標として評価を行った．

最初に，CNRの測定によってCNRが最大となる線質を決定し，次に，決定された条件を中心にいくつかの条件を用いて乳癌の切除標本を撮影し，視認性評価によって診断に最も適した線質を決定した．さらに，CNR測定と切除標本の視認性評価との二つの実験での差異を解明するエッジおよびCDMAMを用いた画質評価実験を追加した．

本研究では，乳癌患者の切除標本を使用して撮影条件を検証するため，研究計画書を当センターの臨床研究審査委員会に提出し承認を得た．また，研究に参加する患者さんには口頭と文書により十分な説明を行ったうえで文書による承諾を得，人権に十分な配慮を行いながら研究を実施した．

1-1 方法1：CNRの測定とCNRが最大となる線質の決定法

CNRの測定はIEC 62220-1-2[12]に規定されている手法により，polymethylmethacrylate(PMMA)を10 mmステップで20～70 mm厚まで変化させたファントムを用い，PMMA上に0.2 mm厚のアルミ板を配置し(Fig. 1)，同じPMMA厚さで平均乳腺線量(average glandular dose; AGD)が一定となる条件で撮影を行った．

CNR測定で用いた画像の前処理方法について説明する．通常のマンモグラフィ装置の場合，数多くの画像処理が加えられた処理済みの画像のみが保存されるシステムになっており，使用者が画像処理の中身を知ることは難しい．本研究を進めるに当たっては，画像処理の影響を排除したうえで研究を進めるため，処理前の画像を評価対象とした．X線が信号として検出されるまでの間には，複数のノイズが信号に重畳される．さらに，X線源と検出器の各素子との距離の違いや，各素子間の成膜状況の違いなどから，信号には均一でない部分(ムラ)があると考えられる．ノイズとムラの除去を目的として，CNR測定には，検出器で検出された処理前の画像に対してオフセット補正とシェーディング補正を行った画像を用いた．測定に先立っては，撮影台の上に何も置かない条件で，X線が照射されない状態の画像を取得し(オフセット画像)，処理前の画像からオフセット画像の値を減算するオフセット処理を施した．さらに検出器表面へのX線の到達線量が5～70 mRとなるようにCNR測定時の値と近い条件で画像を取得し(シェーディング画像)，先にオフセット処理を施された画像からシェーディング画像の値を減算するシェーディング補正を施した．

前処理を行った画像に対し，Fig. 1の四角い点線の枠で囲まれた二つの領域の各々で，画素値QLの平均をとり，アルミ板のない領域の平均値m_{BG}，アルミ板のある領域での平均値m_{AL}を求めた．さらに，それぞれの領域で画素値QLの標準偏差σ_{BG}，σ_{AL}を求め，下の数式(1)に従ってCNRを算出した．

$$CNR = (m_{BG} - m_{AL}) \Big/ \sqrt{(\sigma_{BG}^2 + \sigma_{AL}^2)/2} \quad \cdots\cdots (1)$$

m_{BG}：アルミ板無領域の平均値
σ_{BG}：同　標準偏差
m_{AL}：アルミ板有領域の平均値
σ_{AL}：同　標準偏差

CNR測定で用いた，PMMAの厚みに対する使用ターゲット/フィルタの組み合わせ，管電圧，mAs値，焦点サイズ，AGDの撮影条件をTable 1に示す．撮影は，Mo/Mo，Mo/Rh，W/Rhのターゲット/フィルタの組合せで，23～35 kVの管電圧の範囲で行った．いずれもグリッドを用いた条件下で撮影した．被ばく線量に関してはEuropean Reference Organisation for Quality Assured Breast Screening and Diagnostic Services(EUREF)を参照した[13]．EUREFにはPMMAの厚みごとに，AGDの許容範囲にあるレベルがacceptable levelとして，また，AGDの望ましいレベルがachievable levelとして，それぞれの値が明記されている．一定レベルの画質を確保しながら，被ばくを低く抑えるのが望ましいと考え，CNR測定におけるAGDはEUREFのachievable level(PMMA 20 mm厚で0.6 mGy)に設定した．

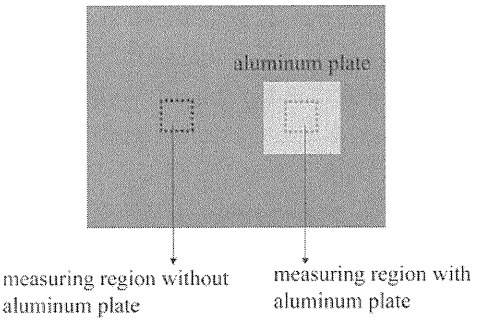

Fig. 1 Experimental setup of PMMA and aluminum plate for measuring CNR.

それぞれのPMMAの厚みで，各ターゲット/フィルタと管電圧の組合せにおけるCNRを測定し，CNRが最大となる線質を決定した．

1-2 方法2：切除標本撮影による最適な線質の検討

前述のように研究への参加に同意を得られた乳癌患者の切除標本を対象として，Mo/Mo，Mo/Rh，W/Rhのターゲット/フィルタの組合せで，26～34 kVの管電圧の範囲でAGDが一定となる撮影条件で撮影した．50症例の切除標本を撮影し，標本厚みが20～70 mmの範囲で10 mm間隔ごとに，できるだけ全摘出の標本を選び，全6標本の46画像を評価し，最適な線質を検討した．本研究では，AGDを一定とし，線質を変えて撮影を行った．管電圧については，実験1の結果からCNRが最大となる管電圧の近傍で設定し，標本の厚みごとに異なる範囲で設定した．AGDはEUREFに記載の方法で導出した[13]．AGDの導出のために取得した半価層のデータをTable 2に示す．切除標本をPMMA板上に置いて撮影を行った．撮影条件は以下のようにして決定した．EUREFには乳房厚みとPMMA厚みとの換算表が示されている[13]．この換算表にはPMMA 1.0 cm厚みごとの値しか記載されていないため，その間の厚みでは線形近似を行

Table 1 Exposure conditions for CNR measurements

Thickness of PMMA (mm)	Target/ Filter	Tube voltage (kV) 23	24	25	26	27	28	29	30	31	32	33	34	35	Focal sizew (mm)	AGD EUREF achievable level (mGy)
		mAs														
20	Mo/Mo	32	24	18	15	12	10	9	7	6	—	—	—	—	0.3	0.6
	Mo/Rh	28	20	15	12	10	9	8	7	6	—	—	—	—	0.3	
	W/Rh	42	32	26	24	20	18	18	16	15	14	—	—	—	0.3	
30	Mo/Mo	—	55	40	32	26	20	16	14	14	12	—	—	—	0.3	1.0
	Mo/Rh	60	40	30	24	20	18	16	14	14	12	—	—	—	0.3	
	W/Rh	80	60	50	44	36	32	30	28	26	24	24	24	—	0.3	
40	Mo/Mo	—	—	—	65	50	40	34	30	28	26	24	—	—	0.3	1.6
	Mo/Rh	—	80	60	46	40	34	30	26	20	24	22	—	—	0.3	
	W/Rh	—	110	90	80	70	60	60	55	46	46	42	38	—	0.3	
50	Mo/Mo	—	—	—	—	100	80	70	65	55	55	50	50	—	0.3	2.4
	Mo/Rh	—	—	110	90	75	65	60	55	50	50	46	44	42	0.3	
	W/Rh	—	—	150	130	110	100	90	80	85	80	75	70	70	0.3	
60	Mo/Mo	—	—	—	—	—	140	130	120	110	110	95	90	90	0.3	3.6
	Mo/Rh	—	—	—	160	130	120	110	100	95	90	85	85	80	0.3	
	W/Rh	—	—	—	—	190	170	150	140	140	130	120	120	110	0.3	
70	Mo/Mo	—	—	—	—	—	280	260	220	220	190	180	170	170	0.3	5.1
	Mo/Rh	—	—	—	—	—	200	180	170	150	140	140	130	130	0.3	
	W/Rh	—	—	—	—	—	—	260	240	220	220	190	190	190	0.3	

Table 2 Data of the half value layer used for this experiment

(Unit: mm)

		Tube voltage (kV) 23	24	26	28	30	32	34	35
Target/Filter	Mo/Mo	0.29	0.30	0.32	0.34	0.36	0.38	0.39	0.40
	Mo/Rh	0.35	0.37	0.40	0.42	0.44	0.45	0.46	0.46
	W/Rh	0.48	0.50	0.53	0.56	0.58	0.59	0.59	0.59

い，乳房厚みを PMMA の厚みに換算した．切除標本の最大厚みを定規で測定した後に PMMA の等価厚みに換算し，その PMMA 等価厚みに，重ねた PMMA 板の厚さを加えた後，トータルの AGD が EUREF の achievable level になるように線質ごとに mAs 値を設定した．その際の mAs は CNR 測定の際に用いた値と等しく，Table 1 に示す値である．

線質検討で用いた画像にも，先の CNR 測定の際と同様に，オフセット補正とシェーディング補正および Log 変換の前処理を施した．また，同じ AGD で撮影条件を変えて測定した場合，処理前の画像には，画素値，コントラスト，粒状性，鮮鋭度などの違いが生じると考えられる．前処理を施すだけでは画質比較が非常に困難なため，標本画像には以下のような後処理を加えた．同一の管電圧と AGD でターゲット / フィルタを Mo/Mo，Mo/Rh，W/Rh と変えて，ある切除標本を撮影した場合の前処理後の画像の 12 ビットでのヒストグラムを Fig. 2a に示す．Mo/Mo から Mo/Rh，W/Rh と線質が硬くなるに従って，透過率が上がるため画素値 QL が上昇し，また，Fig. 2a に矢印で示すように半値幅が狭まることがわかる．半値幅が狭いということは，ヒストグラムにおける左右の階調のピクセルが少ないことを示しており，画像のコントラストが低いこと示している．すなわち，線質が硬くなるほど画像のコントラストが低くなることを示している．コントラストの異なる状態で画質比較を行うのは困難であるため，ある被写体に対して得られた線質違いの画像の階調がほぼ一致するように，画素値 QL の中心値とコントラストを揃える画像処理を施した(Fig. 2b)．具体的には，切除標本の前処理後の画像に対し，切除標本が写っている領域を関心領域とし，関心領域での平均濃度 QL_{ave} と分散 σ を

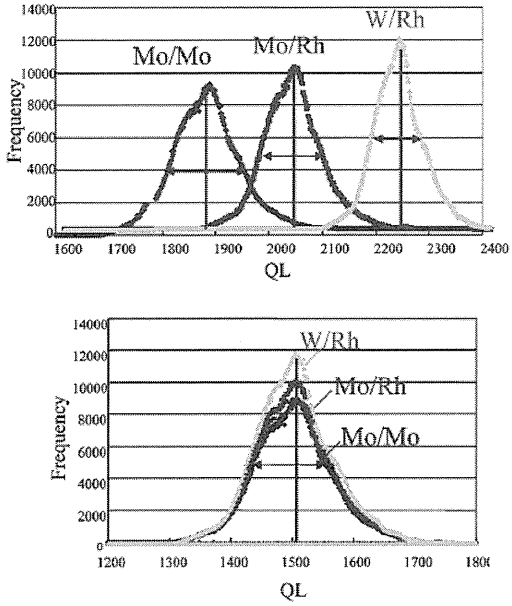

Fig. 2 Image processing and adjustment applied to the breast specimen images.
(a) Unadjusted histogram.
This reveals that the harder the beam quality, the higher the center value (transmission dose increases) and the smaller the distribution value under the consistent AGD (contrast decreases).
(b) Adjusted histogram.
Aligning the distribution and the center values allows the images to have almost exactly the same distribution patterns.

算出した．前処理後の画像に対し，下式(2)の処理を加えた．

$$QL'=a\,(QL-QL_{ave})/\sigma+Q \quad \cdots\cdots\cdots\cdots\cdots\cdots (2)$$

QL'：階調調整後の画素値
a：任意係数
σ：関心領域における画素値の分散
QL：画素値
QL_{ave}：関心領域における画素値の平均
Q：任意画素値

ここで，任意係数 a と任意画素値 Q は，QL' の値が画像診断に適する十分な濃度とコントラストを得られるように適切に設定すればよい．本実験では切除標本画像を12ビットで扱ったため，上限の QL は4095である．切除標本の画像に対し，Fig. 2のようなヒストグラムを取るとやや低 QL 側での頻度が高く，高 QL 側の頻度が低い傾向にあったため，中心値を1500と低めに設定した．また，a については画素値 QL が0を下回ったり，上限値4095を超えないように調整し，全乳房切除標本の全線質の画像において共通の値 a=270，Q=1500を用いた．式(2)の処理を行った後，線質違いの画像の階調処理が揃ったことをヒストグラムにて確認した．以上の階調処理によって線質の違う画像の平均濃度と分散を揃えることができ，画像濃度とコントラストの違いを低減して画質が比較できるようになった．次に，本研究では臨床現場で診断に用いる段階の画像で基本画質や所見の見え方の違いを評価するために，階調を揃えた後，全画像に対し同一の周波数処理を掛けた．周波数処理には当院のFCR PROFECT-CS(富士フイルム社製)で採用してきたマルチ周波数処理(multi-objective frequency processing; MFP)を用いた[14]．このMFPでは周波数強調とダイナミックレンジ圧縮がコントロールされている．全空間周波数成分に対して，バランスよく強調を加え，さらに強い信号で発生するオーバーシュートを抑制する効果がある．

周波数処理は画質に影響するので，どの項目を用いて画質評価を行うかの選択は非常に重要となる．マンモグラフィの臨床画質評価の項目は乳腺濃度，ベース濃度，乳腺内コントラスト，乳腺外コントラスト，粒状性，鮮鋭度，アーチファクトであるが[15]，今回の切除標本画像では階調を揃えているため，濃度，コントラストは同一である．さらに，階調を揃えた後に同一の画像処理を施しているため，アーチファクトの影響は線質の違う画像に対して同一に生じる．したがって，画質評価に必要な評価項目は粒状性と鮮鋭度となる．粒状性と鮮鋭度については，周波数処理の掛け方によってトレードオフの関係があることがわかっている．例えば高周波側の強調を高めると粒状性が悪化する代わりに，鮮鋭度が向上する．したがって，画質評価においては粒状性と鮮鋭度の両方のバランスを評価することが非常に重要である．

前述した同一の画像処理を施した画像をドライイメージャ(DRYPIX 7000，富士フイルム社製)にてフイルムに出力し，シャウカステンにターゲット/フィルタと管電圧が異なる切除標本画像を並べた．乳房の画像診断を専門とする12名の放射線科専門医が，先に説明した粒状性と鮮鋭度の二つの項目についてそれぞれ，Mo/Rh，28 kVでの画像を基準0とし，±5の範囲の目盛りに評価値を記入し，連続値で評価

した．基準画像より良い場合を＋，基準画像よりも劣る場合を－とした．評価の際，それぞれの厚みごとに基準画像(Mo/Rh，28 kV)を含めて比較する全画像が一度にシャウカステンに提示される．評価者は，粒状性，鮮鋭度のそれぞれの項目ごとに序列を付けて画像を並べ直した後，評価値を記入した．先入観が評価に影響しないように，評価者には画像撮影条件は開示されていない．また，他者の評価結果が影響しないように，評価者ごとに評価を行った．さらに，病変部の視認性での検討を加えた．以上の方法で診断に最適な線質を検討した．なお，検体の厚みを得るために，PMMA を 5 mm から 35 mm 追加し，20 mm から 70 mm とした．

1-3 方法 3：鮮鋭度と粒状性の影響を確認するための実験

画像特性に影響する鮮鋭度および粒状性に関して，実験を追加実施した．散乱線の割合はエネルギーが高くなるほど増加する傾向をもつ[16]ため，(1)散乱線の寄与を含めた鮮鋭度に着目した解析を行った．さらに，粒状性による視認性評価への影響を確認するために，(2)CDMAM ファントムによる視認性評価を実施した．

(1)の実験では，まず撮影条件間の AGD が一定となるように鮮鋭度測定用エッジを撮影し，IEC62220-1-2[12]に規定されているエッジ法により modulation transfer function(MTF)を測定した．MTF テストデバイスは 0.8 mm 厚のステンレス板を使用した．Fig. 3a に示す配置で散乱線の影響がほぼない状態での MTF を測定した．次に，Fig. 3b に示す配置で MTF テストデバイスとディテクタ間に 20 mm 厚の PMMA 板を設置し，散乱線のある状況での MTF を，ターゲット / フィルタを Mo/Mo，Mo/Rh，W/Rh と変え，管電圧は一定の 28 kV として測定した．MTF テストデバイスとディテクタ間の距離をとって MTF を測定する方法は一般的には行われない．しかし，実際にマンモグラフィ装置で乳房を撮影する場合，病変部は乳房組織に包まれている場合が多く，病変部が数 10 mm 程度検出器から離れた状態にあることが一般的である．病変部の周りは乳房組織が取り囲み，それが散乱を生じさせる原因になっている．20 mm 厚の PMMA 板は乳房組織を見立て挿入した．この実験では散乱の影響のほかに拡大効果が入るが，Mo/Mo，Mo/Rh，W/Rh の焦点サイズはすべて同一の 0.3 mm であること，さらに，焦点とディテクタ間の距離 650 mm に対して，Mo と W の焦点の位置は 1%程度しか違わないことから，拡大の効果はすべてのターゲット / フィルタでほぼ変わらないと考えられる．したがって，MTF の増減は散乱線の大小を相対的に比較可能であると考えられる．

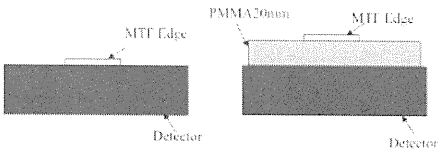

Fig. 3 MTF measurement configuration without PMMA plate (a) and with PMMA plate (b). a | b

続いて行った(2)の実験では，CDMAM ファントムを 20 mm 厚の PMMA の上に置き，さらに CDMAM ファントム上に 10 mm の PMMA を重ね，PMMA 等価厚みを 40 mm とした．ターゲット / フィルタを Mo/Mo，Mo/Rh，W/Rh と変え，管電圧を一定の 28 kV とし，AGD を EUREF の achievable level 1.6 mGy に対して極めて低い 0.9 mGy と少し高い 1.8 mGy となるように二つの AGD 基準値を設け，それぞれの撮影条件下で 8 枚の画像撮影を行った．同一線質で AGD だけを変化させた場合，コントラスト，鮮鋭度は変わらず，粒状性だけが変化することになる．したがって，AGD の違う画像セットを比較することで，粒状性が画質にどう影響し，最適な線質がどう変化するかが分かると予測される．なお，画像は Log 変換した後，前述した前処理と階調処理，さらに周波数処理を施した．3 名の読影者が画像セットの中から 3 枚を任意に抽出し，照度が 50 lx の暗室内で，液晶モノクロ 5 M ピクセル，21.3 型のモニタ(ナナオ社製，RadiForceGS510)にて評価を行った．なお，CDMAM 評価における観察時間には特に制限を与えていない．CDMAM 評価の結果から下式(3)により image quality figure(IQF)を求め，画質の比較を行った[17]．画質が良くなるほど IQF は小さくなる．

$$IQF = \sum_{i=1}^{n} C_i \times D_{i,\min} \quad \cdots\cdots (3)$$

C_i：ディスクの厚さ

$D_{i,\min}$：ディスク直径

n：ステップ数

IQF の統計的有意差検定は t 検定(two-tailed paired t-test)で行い，$p<0.05$ を有意差ありとした．

2. 結 果

CNR 測定結果を示す(Fig. 4)．CNR はすべての厚さで W/Rh のターゲット / フィルタの組合せが最も良かった．PMMA 20 mm ではいずれのターゲット / フィルタにおいても CNR が 13 以上 14 以下の範囲に収まり，ほぼ同等であったが，PMMA 70 mm では

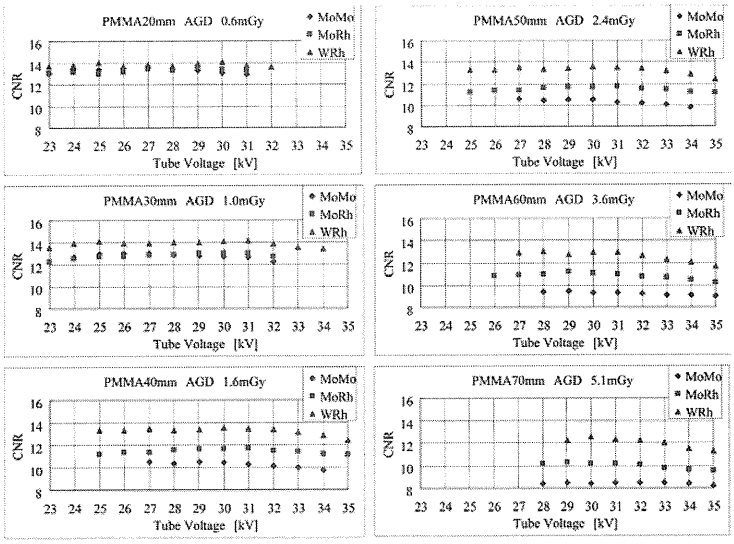

Fig. 4 CNR test results.

Table 3 The average image evaluation score

Thickness (mm)	Tube voltage (kV)	Score of sharpness			Score of graininess			Total score (Sharpness + Graininess)			High scored Target/Filter
		Mo/Mo	Mo/Rh	W/Rh	Mo/Mo	Mo/Rh	W/Rh	Mo/Mo	Mo/Rh	W/Rh	
20	26	1.35	0.75	−0.10	0.45	−0.50	0.20	1.80*	0.25	0.10	
	28	−0.40	0.00	0.60	0.20	0.00	0.25	−0.20	0.00	0.85	Mo/Mo
	31	−0.40	—	—	0.20	—	—	−0.20	—	—	
30	26	−0.35	−0.10	−0.90	−0.15	−0.20	−0.25	−0.50	−0.30	−1.15	
	28	0.75	0.00	−0.20	−0.10	0.00	−0.55	0.65*	0.00	−0.75	Mo/Mo
	30	—	0.20	−0.85	—	−0.10	−0.35	—	0.10	−1.20	
40	28	−0.15	0.00	−1.00	−0.90	0.00	−0.50	−1.05	0.00*	−1.50	
	30	0.00	−0.65	−0.90	−0.55	−1.15	−0.25	−0.55	−1.80	−1.15	Mo/Rh
	32	−0.10	−0.35	—	−0.70	−0.40	—	−0.80	−0.75	—	
50	26	−0.45	−0.45	—	−0.23	0.20	—	−0.68	−0.25	—	
	28	−0.10	0.00	−0.05	0.00	0.00	0.15	−0.10	0.00*	0.10*	Mo/Rh or W/Rh
	30	—	−0.05	0.00	—	−0.20	0.00	—	−0.25	0.00*	
	32	—	0.10	—	—	−0.12	—	—	−0.02	—	
60	28	—	0.00	−0.30	—	0.00	0.30	—	0.00	0.00	
	30	—	0.35	−0.15	—	0.30	0.40	—	0.65*	0.25	Mo/Rh or W/Rh
	32	—	−0.05	0.00	—	0.35	0.50	—	0.30	0.50*	
	34	—	−0.15	−0.15	—	0.25	0.55	—	0.10	0.40	
70	28	—	0.00	—	—	0.00	—	—	0.00	—	
	30	—	−0.30	0.10	—	0.35	0.55	—	0.05	0.65	W/Rh
	32	—	−0.35	0.50	—	0.50	0.45	—	0.15	0.95*	
	34	—	−0.30	−0.05	—	0.55	0.40	—	0.25	0.35	

W/Rh ではCNR が 12 前後で推移する一方，Mo/Mo ではCNR が 9 以下まで低下しており，CNR は PMMA が厚くなるに従ってターゲット / フィルタの違いによる差が広がっていく傾向が見られた．すなわち，W/Rh の組合せでは，PMMA が 20 mm から 70 mm に厚くなっても，CNR は 14 から 12 までしか低下しないが，一方，Mo/Mo の組合せでは，CNR は 13 から 9 まで低下し，W/Rh の組合せは PMMA が厚くなっても CNR の低下を抑えられることが分かった．本測定では，いずれのターゲット / フィルタの組合せにおいても，管電圧を変えた場合の CNR の変化は小さく，最も変化した条件は PMMA 60 mm で W/Rh 28 kV から 32 kV に変えた場合で 9.8%であった．CNR の管電圧に対する依存性は小さいことがわかった．

切除標本の画質評価の結果を Table 3 にまとめる．前述した方法で画像処理によって線質違いの画像の階調を揃えたので，全体コントラストは線質によらず一定である．鮮鋭度の評価値と粒状性の評価値

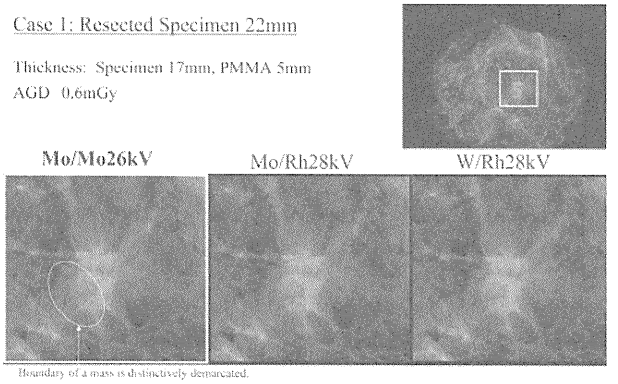

Fig. 5 Images of a resected specimen (22 mm). Because the image obtained using the Mo/Mo combination at 26 kV forms the most distinctive image compared to the other combinations, the density can be differentiated without difficulty. The images obtained using Mo/Rh and W/Rh seem somewhat indistinct.

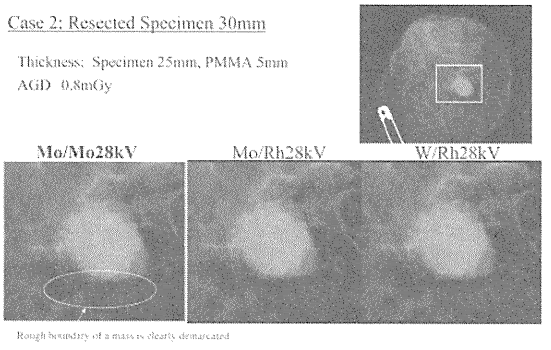

Fig. 6 Images of a resected specimen (30 mm). The best combination for demarcating the boundary of tumors is Mo/Mo. It also makes a distinctive boundary with a mass overlapping a mammary gland.

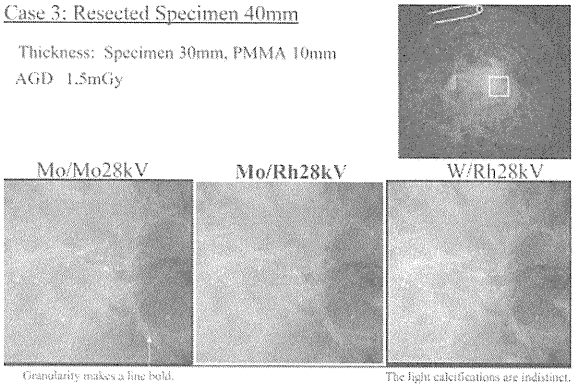

Fig. 7 Images of a resected specimen (40 mm). The granularity of the Mo/Mo image is the worst in this case. The mammary gland in the Mo/Mo image is bolder than that in the images obtained under the other exposure conditions. The amorphous calcifications under the W/Rh combination are less distinctive. The Mo/Rh image visualizes the amorphous calcifications most sharply.

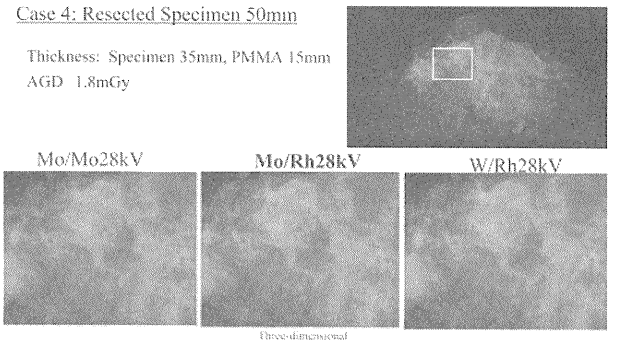

Fig. 8 Images of a resected specimen (50 mm). The image under the Mo/Mo combination has high granularity and seems to lack information. The image under the Mo/Rh combination delivers three-dimensional information because of its lower granularity. In the W/Rh image, the level of granularity is good for recognizing the distinct amorphous calcifications, but the whole image is blurry.

との和で比較すると，標本厚みが 20～30 mm と薄い場合には，Mo/Mo の組合せで最も高く，標本厚みが 40 mm の場合には Mo/Rh の組合せで，標本厚みが 50～60 mm の場合には Mo/Rh または W/Rh で，さらに標本厚みが 70 mm では W/Rh の組合せで高い値となった．

次に，病変部の視認性評価の結果を Fig. 5～9 に示す．切除標本の視認性評価では，標本の厚みが 20～30 mm と薄い場合(Fig. 5，6)には，Mo/Mo の組合せが最も粒状性と鮮鋭度で優れているため，腫瘍辺縁の情報が読みやすく，濃度差がわかりやすかった．Mo/Rh と W/Rh では鮮鋭度が悪いため，腫瘤辺縁の情報が読みにくい画像であった．標本の厚みが 40～50 mm では(Fig. 7，8)，Mo/Mo では粒状性が悪いので，乳腺が太く見え，さらに，淡い石灰化が見えにくくなっていた．W/Rh では，粒状性はよいが鮮鋭度が不足しているので，淡い石灰化や腫瘍辺縁の所見が観察しづらかった．Mo/Rh が粒状性と鮮鋭度ともに最も良いバランスであるので，診断に適していた．60 mm 以上の厚みの標本では(Fig. 9)，Mo/Mo では粒状性が悪く，また Mo/Rh の粒状性も W/Rh に比べるとやや劣るので，あまり診断には向かなかった．W/Rh は粒状性で Mo/Rh よりも圧倒的に良いので，淡く不明瞭な石灰化がよく視認できていた．

以上の切除標本撮影の画質評価と病変部の視認性評価の結果を Table 4 にまとめる．ここで，病変部の見え方が最も良好な条件を○，次に良好な条件を△，最も視認性が悪い条件を×としている．

散乱線の影響を確認するために行った実験の結果を Fig. 10 に示す．散乱線がない状況では，すべての